Journal Pre-proof

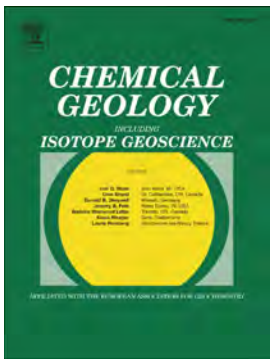

The carbon budget of crustal reworking during continental collision: Clues from nanorocks and fluid inclusions

Gautier Nicoli, Alessia Borghini, Silvio Ferrero

PII: S0009-2541(22)00319-9

DOI: https://doi.org/10.1016/j.chemgeo.2022.121025

Reference: CHEMGE 121025

To appear in: *Chemical Geology*

Received date: 10 November 2021

Revised date: 15 July 2022

Accepted date: 18 July 2022

Please cite this article as: G. Nicoli, A. Borghini and S. Ferrero, The carbon budget of crustal reworking during continental collision: Clues from nanorocks and fluid inclusions, *Chemical Geology* (2022), https://doi.org/10.1016/j.chemgeo.2022.121025

This is a PDF file of an article that has undergone enhancements after acceptance, such as the addition of a cover page and metadata, and formatting for readability, but it is not yet the definitive version of record. This version will undergo additional copyediting, typesetting and review before it is published in its final form, but we are providing this version to give early visibility of the article. Please note that, during the production process, errors may be discovered which could affect the content, and all legal disclaimers that apply to the journal pertain.

© 2022 Published by Elsevier B.V.

Journal Pre-proof

THE CARBON BUDGET OF CRUSTAL REWORKING DURING CONTINENTAL COLLISION: CLUES FROM NANOROCKS AND FLUID INCLUSIONS

Gautier Nicoli[a,*] gautier.nicoli@gmail.com, Alessia Borghini[a], Silvio Ferrero[a,b]

[a]Institut für Geowissenschaften, Universität Potsdam, 14476 Potsdam-Golm, Germany

[b]Museum für Naturkunde (MfN), Leibniz-Institut für Evolutions- und Biodiversitätsforschung, 10115 Berlin, Germany

[*]Corresponding author.

Abstract

The source of volatiles in the continental crust is a long-standing issue. In addition to controlling the amount of melt generated during anatexis, H_2O and CO_2 budgets of the middle and lower siliciclastic crust are also of great importance for carbonate precipitation, ore concentration, orogenic degassing and carbon storage. Here we focus on two case studies of partially melted metamorphic rocks of crustal affinity– the Ivrea Zone in the Western Alps (0.8 GPa) and the Central Maine Terrane (1.8 GPa), USA. These terrains contain fluid inclusions and carbon-bearing nanogranitoids (former melt inclusions) from which the H_2O and CO_2 content has been estimated via nanoscale analyses. Thermodynamic modelling is used to quantify the amount of internally derived, mineral-bound bulk rock CO_2 necessary to reproduce the volatile contents of these melt inclusions. The minimum amount of bulk rock CO_2 present at peak metamorphic conditions is estimated at 400 ppm for the Ivrea Zone and 3000 ppm for the Central Maine Terrane. This suggests that the flux of carbon associated with the burial of siliciclastic sediments in the lower crust during the Phanerozoic is 0.2-4.4 Mt C/yr. These values, as well as the nature of the source of the deep crustal carbon might have changed with time, with periods dominated by internal reworking rather than external inputs. The protracted growth and differentiation of the continental crust through the reworking of supracrustal materials in continental collision settings is a key element of carbon storage processes. The stability of the continental crust through time provides an ultimate, long-lasting reservoir of carbon.

Keywords: Continental crust, garnet, melt inclusions, carbon cycle

1. Introduction

With the advent of plate tectonics at ca. 3.0-3.2 Ga (Dhuime et al., 2015; Hawkesworth & Brown, 2018), critical changes in mantle potential temperature (e.g., Korenaga, 2018; Silver & Behn, 2008) and thickness, thermal state, metamorphic conditions, and compositional variability of the crust (e.g., Condie, 1993; Brown et al., 2020; Hawkesworth & Jaupart, 2021; Palin et al., 2020) are thought to have led to different, more efficient, mechanisms for the recycling and reworking of supracrustal material into the mantle and the crust. The progressive storage of surface-derived volatile elements

(e.g., H, C, N, F) into the solid Earth might have in turn helped to modify the physicochemical properties of Earth's fluid envelopes, i.e., hydrosphere and atmosphere (Foley, 2015), thus establishing a global feedback loop between deep Earth processes and surface cycles, promoting the development of life (e.g. McCulloch, 1993; Kramers, J. D., & Tolstikhin, I. N., 1997; Gerya et al., 2020; Nicoli & Ferrero, 2021).

In the modern Earth, endogenic and exogenic fluxes of water and carbon primarily take place in convergent settings (e.g., subduction zones, arc volcanoes), extensional settings (e.g., mid-oceanic ridges, back arcs, rifts), and hotspots (e.g., Kelemen & Mannings, 2015; Wong et al., 2019; Korenaga et al. 2017; Bekaert et al. 2021; Rüpke et al., 2004; Zellmer et al., 2017). Plank & Manning (2019) have suggested that the sequestration of carbon in the solid Earth (82 ± 14 megatons of carbon per year - Mt C/yr), is currently balanced by carbon degassing (79 ± 14 Mt C/yr). However, significant uncertainties still remain, partially due to the fact that these fluxes may vary both in time and space (e.g., Plank & Manning, 2019; Stewart et al., 2019). Additionally, differences in the time-scales at which these exchanges occur, and how long the carbon might remain in a specific reservoir (Lee et al., 2019) complicate the comparisons between the different storage units/mechanisms that constitute the global carbon cycle. Based on paleo-reconstructions of plate boundaries, Wong et al. (2019) have shown that, overall, net carbon outgassing prevailed in the past 200 Ma, highlighting the need for an additional surface sink and/or deep lithospheric storage in the upper mantle and lower crust. Although continental and seafloor weathering can temporally maintain the global balance of the carbon cycle through negative feedback (Berner & Caldeira, 1997; Catling & Zahnle, 2020), up to 70% of the carbon contained in the sediments will be ultimately redistributed to the atmosphere during crustal recycling and reworking (Stewart & Ague, 2021; Martin & Hermann, 2018). Therefore, the secular decrease in the atmospheric partial pressure of carbon dioxide, pCO_2 (Catling & Zahnle, 2020) would require the existence of a long term reservoir. The preservation and stability of granulitic terrains through time (e.g., Harley, 1989; Brown & Johnson, 2019) and the current estimated budget of the igneous and metamorphosed continental crust, (~10^7 gigaton of mineral-bound carbon (Gt C) - Wedepohl, 1995), suggest that the lower crust, and to some extend the upper lithospheric mantle (Kelemen & Manning, 2015), may be such reservoirs. Although the recycling of carbon through subduction has been the focus of numerous studies (e.g., Dasgupta & Hirschmann, 2010; Kelemen & Manning, 2015Plank & Manning, 2019), the impact of crustal reworking is often left out of the equation (Nicoli & Ferrero, 2021).

In this contribution we investigated the impact of crustal reworking, i.e., erosion, sedimentation, burial and partial melting of sediments, on the carbon budget of collisional orogens in the deep crust and how these processes can be tied into the evolution of the global carbon cycle. We showed that primary melt inclusions in peritectic garnet in granulitic rocks of crustal affinity can be used to quantify the amount of surface-derived carbon that survive decarbonation and is ultimately stored in the roots of mountain belts. The data used in this paper derive from experimentally

rehomogenised melt inclusions that then have been measured with the nanoscale secondary ion mass spectrometry (NanoSIMS) for CO_2 and H_2O content.

2. Nanorocks and fluid inclusions in garnet

The recognition and study of preserved, primary multiphase solid inclusions in peritectic minerals in high-grade metamorphic rocks evolved from a limited and exotic approach (Cesare, 2008; Cesare et al., 2009) to one of the main staples of the field targeting the role of partial melting in crustal differentiation (Bartoli, 2021 and references therein). A decade-long research effort involving multiple researchers has shown beyond doubt how these inclusions, often crystallised to "nanorocks" (Bartoli & Cesare, 2020), allows us to access pristine melt compositions trapped at depth during the crustal reworking of a large variety of rocks (Nicoli & Ferrero, 2021 and references therein). While few studies have so far identified mafic rocks hosting crustal melts as inclusions (Ferrero et al., 2021b; Gianola et al., 2022, Nicoli et al., 2022b), in some cases of clear metasomatic origin (Borghini et al., 2022), the large majority of the data available on nanorocks comes from metasedimentary rocks (~70% of the most up-to-date dataset, Nicoli & Ferrero 2021).

The development of new analytical protocols for NanoSIMS analyses allow us to estimate the concentration of H_2O and CO_2 in primary melt inclusions trapped in garnet, one of the most common peritectic phases during mica breakdown, fluid-absent partial melting of crustal rocks at peak metamorphic conditions (e.g., Bartoli et al., 2014; Acosta-Vigil et al., 2016; Ferrero et al. 2021a and references therein). Carbon-bearing melt (MI) and fluid (FI) inclusions exist in many high-grade terrains (Nicoli & Ferrero, 2021). However, there are to date only four terrains in which the volatile content of anatectic melts has been determined: the Ivrea Zone granulites (Carvalho et al., 2019); the Central Maine Terrane (Ferrero et al., 2021a); the Gruf Complex (Gianola et al., 2021) and the Edixon Metamorphic Complex (Ferri et al., 2020). Among them, the best suited case studies to investigate the mobility and budget of carbon during crustal melting in a crustal thickening environment (Barrovian series - 350-750 °C.GPa^{-1} – Brown, 2006) are the granulites from the Ivrea Zone and the Central Maine Terrane. Here, multiphase solid inclusions have been confidently recognised to be derived from the partial melting of a graphite-rich and, in the Ivrea case only, carbonate-rich siliciclastic metasedimentary rocks. We detail below their metamorphic history as well as their MI and FI compositions.

The Ivrea Zone is located in the western part of the Italian Alps and represents a fragment of the mid to lower Permian continental crust metamorphosed at ca. 270 Ma (Schmid & Wood, 1976; Schmid, 1993). The studied samples come from the supracrustal Kinzigite Formation of the Val Strona di Omegna. The Kinzigite Formation comprises of mainly metapelites, interlayered with marbles, quartzites and metabasites (Quick et al., 2003; Schmid, 1993). Metapelitic samples were

collected in the three different metamorphic zones: upper amphibolite facies, transition zone and granulite facies (Carvalho et al., 2019). Both peak pressure and temperature (P-T) conditions increase from SW to NE as the metamorphic grade and they range from 640 - 710 °C and ~0.4 - 0.8 GPa in the upper amphibolite facies to 830 – 910 °C and ~ 0.9 - 1.1 GPa in the granulite facies (Redler et al., 2012; Ewing et al., 2013). In the upper amphibolite facies zone, the samples are metatexites with a melanosome containing biotite, sillimanite, quartz, plagioclase, garnet, K-feldspar and minor muscovite (Carvalho et al., 2019). In the transition zone, the samples are stromatic metatexite with a melanosome constituted of biotite, garnet, sillimanite, K-feldspar, plagioclase and quartz (**Fig. 2a**). The granulite facies zone contains instead diatexites with abundant quartz, K-feldspar, plagioclase, garnet, sillimanite and minor biotite (**Fig. 2b**). Graphite is present as accessory mineral in all these rock types and garnets contain clusters of nanogranitoids, i.e., crystallised melt inclusions with a granitoid composition, and fluid inclusions concentrated mostly in the inner part (**Fig. 2 a-b**). Nanogranitoids (**Fig. 2c**) contain mainly K-feldspar (rarely its hexagonal polymorph kokchetavite), plagioclase or its orthorhombic polymorph kumdykolite, quartz (or cristobalite/tridymite), biotite, muscovite, chlorite and locally calcite, CH_4 and N_2 (Carvalho et al., 2019, 2020). The H_2O and CO_2 content in the melt trapped in the different rocks is 5 - 10 wt.% and 500 - 2400 ppm respectively. The fluid inclusions (**Fig. 2c**) contain both fluid and solid phases: the fluid portion consists of CO_2, CH_4 and N_2 in variable amounts, whereas the most common solid phases are siderite and pyrophyllite with minor occurrence of kaolinite, calcite, magnesite and graphite (Carvalho et al., 2019, 2020).

The Central Maine Terrane is located in the north-eastern part of Connecticut. Peak metamorphism took place at ultra-high temperature (UHT) and high pressure (HP) conditions, T = 1050 °C and P = 1.7 - 2 GPa (Ague et al., 2013; Axler & Ague, 2015; Keller and Ague, 2018) around 380 Ma during the Acadian orogeny (Robinson et al., 1998; van Staal et al., 2009). These metamorphic estimates are consistent with the orogenic plateau model such as the Himalayas, predicting UHT conditions (T > 900 °C - Harley, 1998) in the lower crust (e.g., Jamieson et al., 2004; Hillenbrand et al., 2021). The samples hosting inclusion-rich garnets are schists characterised by garnet, sillimanite, K-feldspar, plagioclase, quartz, cordierite and biotite (Axler & Ague, 2015) (**Fig. 2d**). Graphite and resorbed biotite occur as inclusions in garnet, along with thin rutile needles interpreted as exsolutions (Axler & Ague, 2015). Their protolith has been identified as an aluminous or volcanoclastic sediment deposited along with black shale in a syn-tectonic marine basin at the forefront of the orogen (van Staal et al., 2009; Ettensohn et al., 2019; Hillenbrand, 2020). Differently from the Ivrea Zone samples, here garnets contain clusters composed only of nanogranitoids (**Fig. 2 f**) charaterised by cristobalite, phlogopite, white mica, an unidentified feldspar-like phase with main Raman peak at 430 cm^{-1} and accessory apatite and ilmenite (Ferrero et al., 2021a). The H_2O content is in average ~ 4 wt.% whereas CO_2 is in average ~ 3100 ppm, the highest values compared to the other case studies (Ferrero et al., 2021a). A feature so far unique observed here is the very high halogen content of the nanogranitoids, with both Cl and F near 1 wt.% in some cases, providing novel clues on

the connection between crustal melting and the formation of F-rich ore forming fluids (Lamadrid & Steele-MacInnis, 2021).

3. Modelling

3.1. Set-up

In order to quantify the amount of bulk rock H_2O and CO_2 necessary to reproduce the volatile content of anatectic melt inclusions at peak metamorphic conditions, we used averaged siliciclastic sediment compositions most likely to represent the protoliths of the investigated metasedimentary granulitic rocks. The shale composition from Ague (1991) represents the inferred protolith for the granulites in the Ivrea Zone and a greywacke composition (Pettijohn, 1963) represents the protolith for the Central Maine Terrane (**Table 1**). We used rhyolite-MELTS v.1.1.0 (Gualda et al., 2012; Ghiorso et al., 2015), which includes a non-ideal CO_2 - H_2O fluid model (Duan and Zhang, 2006), in the MnO - Na_2O – CaO – K_2O – FeO – MgO – Al_2O_3 – SiO_2 – H_2O – TiO_2 – O_2 - CO_2 (NCKFMASHTC) along prograde Barrovian P-T paths, from 700°C and 0.5 GPa to 900 °C and 1.15 GPa for the Ivrea Zone, and from 700°C and 1.2 GPa to 1050 °C and 1.8 GPa for the Central Maine Terrane. Peak metamorphism is followed by isothermal decompression to 0.7 and 1.0 GPa respectively. Modelling was run for a set of different CO_2 and H_2O contents. Bulk H_2O varies from 1 to 3 wt.%, which represent the range of mineral-bound water at amphibolite facies conditions, i.e., pre-partial melting (Ague, 1991) and necessary for water-saturated solidus conditions (e.g., Nicoli & Dyck, 2018). Bulk CO_2 varies from 0.01 to 0.6 wt.%, which is similar to the average content suggested by Chu & Ague (2013), 0.2 - 0.3 wt.%, for a sub-carbuminous metapelitic composition (see discussion). As the bulk CO_2/H_2O ratio in siliciclastic rocks rarely exceed 0.25 (Ague, 1991), except in terrigenous-carbonate mixes found subduction zones (Plank & Langmuir, 1998), we did not model scenarios for which the amount of bulk CO_2 exceeded the amount of bulk H_2O.

3.2. Results

3.2.1. H_2O and CO_2 content

In the Ivrea Zone (**Fig. 3a**), the modelled melt volatile concentrations match the average measured CO_2 and H_2O concentrations of rehomogenised MI for the following bulk compositions: H_2O = 1 wt.% and CO_2 = 100 - 300 ppm; H_2O = 2 wt.% and CO_2 = 200 - 500 ppm; H_2O = 3 wt.% and CO_2 = 200 - 800 ppm. The apparent increase in bulk CO_2 concentration between the transition and granulite zone supports the idea of greater CO_2 solubility in melt at higher temperature. Importantly, as pointed

out by Carvalho et al. (2019), the range of CO_2 values for the three metamorphic zones is very similar and clear distinction between carbon content and peak P-T conditions cannot be drawn with certainty.

In the Central Maine Terrane (**Fig. 3b**), the modelled melt volatile concentrations match the average measured CO_2 and H_2O concentration of rehomogenised MI for the following bulk compositions: H_2O = 1 wt.% and CO_2 = 100 - 2000 ppm; H_2O = 2 wt.% and CO_2 = 200 - 4000 ppm; H_2O= 3 wt.% and CO_2 = 300 - 6000 ppm. The rehomogenised MI with the lowest H_2O and CO_2 content – 1.64 wt.% and 113 ppm, respectively, is the result of fluid loss (Ferrero et al., 2021a) and should not be considered in assessing the bulk volatile content.

The modelling shows that these volatile-bearing inclusions form along the prograde path or at near peak metamorphic conditions. This is in agreement with the spatial distribution of inclusions in garnets(**Fig. 2**) as their occurrence in the core of the mineral supports growth of the host phase and entrapment during the prograde history of the rocks. The presence of COH-fluid in equilibrium with anatectic melt at 700 - 750 °C (Fig. 3a) in the Ivrea Zone is consistent with melt + fluid entrapment during garnet formation, thus indicating that melt and fluid entrapment must occur during the early stage of partial melting.

3.2.2. Major element chemistry

Major element chemistry were used to narrow down the bulk H_2O values needed to reproduce the volatile content of the melt. For a fixed amount of bulk H_2O, the different concentrations of bulk CO_2 gave similar melt compositions. Therefore, the paths displayed in Figure 4 represent average paths for the different water content.

In the Ivrea Zone, the average major element composition of the rehomogenised melt inclusions is of peraluminous affinity, characterised by an average composition of SiO_2: 68 ± 2 wt.%; ASI (ASI = Al/[Ca+Na+K]): 1.9 ± 0.3; AI (AI = Al – [Na+K]): 0.15 ± 0.04; Ca/[Ca+Na]: 0.3 ± 0.1 and Mg#: 0.25 ± 0.08 (**Fig. 4a**). As for the volatile elements, it is difficult to make a distinction between the different metamorphic zones. Carvalho et al. (2019) suggested that the spread of compositions observed in Figure 4a could have resulted from disequilibrium due to the sluggish diffusion of Si and Al versus rapid diffusion of alkalis in the anatectic melt (e.g., Acosta Vigil et al., 2016). In the Central Maine Terrane, the average major element composition of the rehomogenised melt inclusions is also of peraluminous affinity. The granitic melt is characterised by an average composition of SiO_2: 69 ± 2 wt.%; ASI: 1.3± 0.2; AI: 0.06 ± 0.02; Ca/[Ca+Na]: 0.15 ± 0.1 and Mg#: 0.23 ± 0.06 (**Fig. 4b**). For both granulitic terrains, the model with bulk H_2O concentration of 3 wt.% shows best fit with the measured melt inclusions composition along the prograde path and at peak metamorphic conditions.

4. Discussion

Journal Pre-proof

4.1. The CO_2 content of anatectic melts

Devolatilisation of siliciclastic lithologies controls the amount of mineral-bound H_2O available during partial melting (Nicoli & Dyck, 2018 and references therein) and it is of great importance for carbonate precipitation (e.g., Ague, 2000; Lyubetskaya & Ague, 2009), ore concentration (Stepanov, 2021) and release of orogenic gases back to the atmosphere (Stewart & Ague, 2018). During regional, prograde metamorphism, H_2O release from supracrustal rocks is a progressive, multi-step process resulting from the breakdown of chlorite and micas (e.g., Kerrick & Connolly, 2001; Nicoli & Dyck, 2018). The release of CO_2 from metamorphic rocks occurs instead over a relatively narrow temperature window, resulting in a single major episode of metamorphic decarbonation (**Fig. 5**). At amphibolite facies conditions the consumption of carbonates (e.g., calcite, dolomite) and quartz produce CO_2 and a silicate phase (e.g., Ferry, 1988). Consequently, while some of the water survives the main devolatilisation reactions by remaining mineral-bound, most of the CO_2 would partition into a highly mobile fluid phase, supporting the assumption that a significant fraction of the bulk rock CO_2 is leached out of the crust prior to partial melting. Ague (2003) showed that calc-silicates and carbonates lose > 70 % and 20-30 % of their mineral-bound volatile content, respectively, during prograde metamorphism.

A key question that remains, however, is what fraction of the carbon survives the decarbonation reactions and becomes the source of the carbon mobilised during partial melting? Chu & Ague (2013) have showed that between 700 °C and 800 °C, the anatectic melt generated by the partial melting of a graphite-bearing sub-aluminous metapelite at mid-crustal pressure (0.8 GPa) can contain between up to 1500 - 2500 ppm of internally derived CO_2. This is within the range of what Carvalho et al. (2019) measured in the melt inclusions from the Ivrea Zone, 1149 ± 486 ppm. Instead in the Central Maine Terraine the highest melt inclusions CO_2 concentrations, 8109 ppm (Ferrero et al., 2021a), agrees with greater CO_2 solubility at depth (e.g., Brooker et al., 1999, Baker & Alletti, 2012; Yoshioka et al., 2019). It is possible that the span of measured CO_2 values (**Fig. 3**) in both terrains modelled in this paper might be the results of "mosaic" equilibrium related to the heterogeneous distribution of graphite in the protolith (Bartoli et al., 2014). Therefore, we also refer to the average value for the Central Maine Terrane, 3072 ± 2882 ppm CO_2 in the anatectic melt. Our modelling suggests that the volatile content of the melt can be produced internally by considering a siliciclastic sedimentary source containing 3 wt.% of mineral-bound H_2O and a minimum of mineral-bound CO_2 of ~ 400 ppm at 1.1 GPa (in the Ivrea Zone) and ~ 3000 ppm at 1.8 GPa (in the Central Main Terrane). Chu & Ague (2013) calculated similar bulk rock CO_2 concentrations, 200 - 300 ppm, at 0.7 - 0.8 GPa and 700 - 800 °C.

Although we are limited by the number of studies, there is an apparent correlation between the amount of CO_2 that can be retained in the system, pressure and the composition of the starting material (e.g., Holtz, 1995; Martin & Hermann, 2018; Yoshioka et al., 2019; Solomatova et al., 2020).

Silicate melts from crustal anatexis show a positive correlation of CO_2 concentration with depth, similarly to mafic and intermediate melts (Yoshioka et al., 2019). This relationship also extends to greater depths. Recent work on crustal melts trapped in UHP eclogites garnets (~ 4.5 GPa) report the presence of ~ 25,000 ppm of CO_2 (Borghini et al., 2022), one order of magnitude higher than melts formed at 1.0 GPa.

The volatile solubility in melts is an important issue for partial melting processes in the continental crust as it affects the chemical and rheological properties of the resulting magma (Holloway, 1976; Wyllie, 1977, Peterson & Newton, 1989; Clemens et al., 1997). The distribution of CO_2 between the fluid phase and the anatectic melt directly influence the a_{H_2O} of the liquid, displacing the melting reactions in the pressure-temperature space (Thompson & Tracy, 1979). For instance, segregation and channelisation of CO_2-rich fluids might trigger local dehydration of the surrounding lithologies (Touret 1971; Collerson & Fryer 1978; Newton et al. 1980), classically used to explain the origin of charnockites (e.g., Glassley, 1983; Stähle et al., 1987; Dunai & Touret, 1993; Huizenga and Touret, 2012). However, Kempton et al. (1991) showed that a large influx of CO_2 in the lower crust would tend to rehomogenise oxygen isotope, which not the case in most granulite terrains. Recent observations also suggested that a large influx of CO_2-rich fluid is not required for the genesis of these UHT rocks (Fitzsimons et al. 2018). In this scenario, the low a_{H_2O} of fluid inclusions usually observed in charnokites might form as the result of low CO_2 solubility in the melt. Hence, in a heterogeneous lower crust and in the case of an internally derived carbon source, the amount of COH-fluid and its capacity to flux through the different crustal level depends on CO_2 solubility in the anatectic melts. Holtz et al. (1995) suggested that there is a pressure-driven positive temperature response of the water and volatile content in melts. For high thermobaric gradient (T/P) values, solubility is low, suggesting that volatiles mainly concentrate in the gas phase (Cesare et al., 2007). For low T/P values, higher fluid density together with increase in temperature favor CO_2 dissolution into the melt. Therefore, because of greater mobility of the gas phase, carbon loss through devolatilisation in low pressure partially melted rocks would dominate. On the other hand, in high-pressure migmatites, its higher solubility in melts could bring a substantial amount of carbon to the root of mountain belts.

Despite greater solubility at depth, the relatively small concentration of CO_2 available during partial melting does not affect the volume of melt produced, as previously suggested by Clemens & Watkins (2001). The modelling indicates in fact a reduction of only 1% of the melt volume in the CO_2-present scenarios. Therefore, a discrete, internally derived COH-fluid phase is likely to exist in equilibrium with anatectic melt. This indicates that fluid-present partial melting is likely a common feature in the metasedimentary lower crust, however, perhaps not to the extent suggested by Sawyer (2010) and Weinberg & Hasalova (2015).

4.2. Reworking of metasediments

Journal Pre-proof

Although the proportion of metasedimentary rocks in the lower crust is often interpreted to be small compared to the volume of igneous material (Rudnick & Gao, 2003; Huang et al., 2013), it remains of primary importance for two crucial reasons.

First, their presence highlights the relationship between surface material and orogenic granites during crustal differentiation. Weathering of the continental crust and accumulation of sediments in the passive margins and foreland basins constitute a sink for atmospheric carbon (Gaillardet et al., 1999; Berner & Kothavala, 2001). In collisional settings, this material is remobilised during crustal thickening, bringing substantial amount of mineral-bound water and carbon dioxide to deep crustal levels (e.g., Nicoli and Dyck, 2018; Nicoli & Ferrero, 2021). The global compilation of bulk-rock CO_2 concentrations in siliciclastic sediments and their metamorphic equivalent shows a systematic decrease of CO_2 concentration with metamorphic grade (**Fig. 5**). As described above, the main CO_2 loss event occurs at the greenschist-amphibolite facies transition. However, further increases in temperature do not seem to significantly affect the volume of CO_2 retained in the lower crust as amphibolite and granulites display similar concentrations. The modelled granulitic rocks from our study fall within the observed range (**Fig. 5**). The partial melting of metamorphosed siliciclastic sediments ultimately leads to the formation of S-type granites (Clemens, 2006 and references therein). Those granites, and the measured melt inclusions in the granulites reported here, contain comparable concentrations of bulk rock CO_2 suggesting that, to some degree, internally derived carbon finds its way to mid- and upper crustal level. The chemical links existing between the protolith, the migmatites and the resulting granites (Nicoli et al., 2017; Clemens, 1990, 2006; Clemens et al., 2020) hence raises the question of the origin, distribution and budget of the internally derived carbon in the lower and mid-continental crust (see next section).

Second, metasedimentary rocks could overall carry more volatiles than their igneous counterparts. In subduction zones, sediments represent less than 2 % of the volumetric amount of buried material but account for ~ 60 % of the carbon recycled into the mantle (Dutkiewicz et al., 2017; Wong et al., 2019; Kelemen & Manning, 2015; Plank & Manning, 2019). In collisional settings, the material accumulated in the orogenic wedge has a thickness that can exceed 10 km, due to subsidence and repeated stacking (Francu et al., 2002, Stockmal et al., 1986 Hillenbrand et al. 2021). Considering a current reworking rate of 1 km^3/yr (which includes e.g., erosion, sedimentation, and partial melting - Guo & Korenaga, 2020), an average rock density of 2700 kg/m^3 and a CO_2 content of siliciclastic sediments of 0.1 - 4.0 wt.% (**Fig. 5**), the volume of buried orogenic carbon could vary significantly from 0.7 Mt C/yr to 30 Mt C/yr. If we also consider the ~ 7 Mt C/yr derived from carbonates and organic matter from the buried passive margin (Clift, 2017), the maximum flux of carbon during continental collision could add up to 37 Mt C/yr (**Fig. 6**), a flux superior to what is currently released from mid oceanic ridges (16 Mt C/yr) and arc volcanoes (23 Mt C/yr) (Plank & Manning, 2019).

Orogenic belts are also known to be a major emitter of carbon (e.g., Becker et al., 2008; Evans et al., 2008; Groppo et al., 2018; 2021; Menzies et al., 2018; Stewart & Ague, 2018). Stewart et al.

(2019) showed that continental collision currently releases 3-25 Mt C/yr through decarbonation reactions of either carbonates, organic sediments, sedimentary, igneous and/or mantle rocks (**Fig. 6**). Additionally, infiltrations of water-bearing fluids either meteoric (e.g., Newell et al., 2008; Menzies et al., 2016) or derived from the devolatilisation of siliciclastic rocks (e.g., Ague, 2003; Nicoli & Dyck, 2018; Groppo et al., 2021) in the upper part of the crust might lower down decarbonation temperature (Ferry, 1988; Tracy et al., 1983). This would lead to the release of a significant amount of CO_2 at the deformation front of some orogenic belts during the early stage of prograde metamorphism (Stewart & Ague, 2018). Assuming that 20-30 % mineral-bound carbon in carbonate and organic matter and 70 % mineral-bound carbon in siliciclastic sediments is lost during prograde metamorphism (Ague, 2003), we calculated that the exogenic flux towards the surface would be 2-23 Mt C/yr, similar to what has been proposed by Stewart et al. (2019). This suggests that ~ 5 Mt C/yr derived from carbonate and 0.2-9 Mt C/yr derived for siliciclastic sediments could eventually reach lower crustal levels.

At similar reworking rates (Guo & Korenaga, 2020) and considering that our modelling indicates that 0.02 to 0.6 wt.% of CO_2 could be present during the partial melting of sedimentary granulite, we calculate a flux of 0.2 - 4.4 Mt C/yr to the lower crust (**Fig. 6**). The melt fractions generated in the deep crust will eventually gather in a network of leucosomes to feed S-type granites. Based on chemical mass balance between melt, leucosome and residuum, Nicoli et al. (2017) have argued that at least 88 % of the anatectic melt derived from siliciclastic sediments leaves the lower crust before/at peak metamorphism, thus suggesting that the volume of carbon lost to middle and upper crust intrusions equals 0.18-3.8 Mt C/yr. Therefore, the balance of the orogenic carbon cycle relies both on the nature of the buried protolith and the thermal state of the orogen. This balance can be achieved in a relatively closed system, i.e., burial, degassing and partial melting of sediments. However, mantle-derived fluid might significantly increase the flux of carbon in the root of the orogen (Kelemen & Manning, 2015). To decipher the variable nature of the carbon fluxes, both internal and external derived, we looked at the relationship between the source of carbon and plate tectonics throughout Earth's history.

4.3. Sources of carbon and plate tectonics

The source of carbon in the lower crust, and fluids in general, is a long-standing issue (e.g., Aranovich et al., 2016; Clemens et al., 2016). We have shown that the presence of a small fraction of internally derived COH-fluid might be present during partial melting. The reduction of Fe^{3+} and carbon oxidation during mica-breakdown partial melting could be a possible internal source of CO_2 in collisional settings (e.g. Hollister, 1988; Cesare, 2005). However, in accretionary settings, the presence of COH(N)-fluids in UHT granulitic terrains is often seen as the result of the percolation of

invasive mantle brines (e.g., Touret & Huizenga, 2011; 2012; Santosh & Omori, 2008; Sawyer, 2010; Weinberg & Hasalova, 2015; Aranovich et al., 2014; Newton et al., 2014; Touret et al., 2016). Such hypothesis is based, in part, on electrical conductivity studies which have revealed large anomalies attributed to the presence of graphite films in the lower crust (Glover, 1996). The source of the carbon for these deep crustal deposits has been commonly attributed to the flux of external, crustal or mantle-derived, fluids during exhumation (e.g., Jackson et al., 1988; Newton et al. 1980; Touret, 1992; Glover, 1996; Santosh & Omori, 2008; Chu & Ague, 2013). However, the abundance of graphite in the granulitic lower crust is controlled by a diverse set of parameters such as fluid flux, P-T conditions, f_{O_2} (Huizenga & Touret, 2012), and, therefore, cannot be alone indicative of the original carbon budget of the source rock.

Although most of the CO_2 present in the lower crust is thought to be mainly the consequence of mantle degassing (Touret et al., 2016 and reference therein), the compilation of isotopic data on deep crustal carbon-bearing phases indicates that the origin of dense CO_2 rich fluids in granulitic terrains is more contrasted than previously thought (e.g. Touret & Huizenga, 2020). The $\delta^{13}C$ isotopic composition of graphite, fluid inclusions, cordierite (Vry et al., 1990; Peck, 2016) and diamond (Dobrzhinetskaya et al., 2010) present in granulitic rocks indicates that half of the carbon displays an organic signature ($\delta^{13}C < -20\ ^{0}/_{00}$), while the other half indicates a mantle origin ($\delta^{13}C$ 0 to $-10\ ^{0}/_{00}$) (**Fig. 7a**). Historically, most of the isotopic work on fluid inclusions has been carried out in two main locations, the southern tip of India - 0.5-0.6 Gyr, (e.g Baiju et al., 2005; Hoernes et al., 1994; Hoffbauer et al., 1994; Santosh & Wada, 1993; Sanyal et al., 2009; Santish-Kumar, 2000; 2005) and the Western Gneiss Region, Norway - 0.9 - 1.1 Gyr, (e.g., Broekmans et al., 1994). More recent work has also been conducted in Brazil - 0.6.-0.7 Gyr, (e.g., Miranda et al., 2019), South Africa - 2.7 Gyr, (e.g., Safonov et al., 2018) and the Neoarchean Lewisian Complex 2.7 Ga (Parnell et al., 2021) (see supplementary information). A mantle origin for the carbon has been suggested for all of these terrains, associated with, in some cases, some degree of mixing with crustal graphite (e.g., Touret & Huizenga, 2020). This flux of mantle carbon in the lower crust has been regarded as a direct consequence of plate tectonic mechanisms (Santosh & Omori, 2008; Huizenga & Touret, 2012). The advocating authors suggested that decarbonation of subducted slabs from the Archean would have progressively enriched the lithospheric mantle in CO_2. Kelemen & Manning (2015) suggested a current flux of 0-47 Mt C/yr to the conductively cooled mantle and the crust. Such hypothesis is based on two assumptions; that (1) carbon-rich fluids can physically traverse the different layers of the continental crust (Santosh & Omori, 2008), and that (2) long-lasting subduction mechanisms might have been present since the Archean (Palin et al., 2020 and references therein).

The first assumption is supported by the fact that porosity wave transfer under active stress, e.g., deep crustal shear zone, has been shown to be a viable process to explain the migration of carbon-rich fluids through the crust (e.g., Okudaira et al., 2017). However, such phenomenon might likely occur during crustal thinning and retrograde metamorphism (for instance on decompression)

and therefore cannot account for the fluid trapped during the formation of prograde and peak metamorphic minerals, e.g., garnet. In fact, most of the studied inclusions in the literature are often hosted in minerals likely to belong to the retrograde mineral assemblage such as quartz. Because of the occurrence of processes such as multiple CO_2 infiltrations (Huizenga & Touret, 2012) – i.e., CO_2 derived from an external source or from the surrounding rocks - and consumption of graphite and water loss during decompression (Hollister, 1988), these COH-rich fluid inclusions cannot be used alone to decipher with certainty the origin of carbon in the lower crust. Even in garnet, primary fluid inclusions often display a metastable assemblage, indicating a change in their nature between entrapment and cooling due to reaction with the host (Carvalho et al., 2020). Conditions at the base of the continental crust are also critical. The permeability of the Moho to CO_2 fluids increases with temperature and decreases with pressure (Bucher-Nurminem, 1990). In order to affect partial melting processes in the lower crust, the flushing mantle fluid needs to contain more than 70 mol.% of CO_2, which is achieved for Moho temperature > 900 °C at 30 km depth. An alternative mechanism for the transport of crustal carbon during prograde metamorphism would be compaction-driven fluid flow (Tian & Ague, 2014; Tian et al., 2018). This mechanism requires an external heat source and strong channelisation at the base of the crust. Therefore, we do not discard the presence of a free COH-fluid phase during partial melting in granulite terrains, but we suggest instead that external carbon fluid fluxes might only affect specific settings such as some UHT granulite terrains and/or arc granulite where the input of mantle-derived material could provide the necessary heat and volatile input (Collins et al., 2016, 2021; Plank et al., 2013). The mechanism responsible for controlling the carbon budget might therefore be different for distinct periods of Earth history.

As for the second assumption that subduction has been active since the Archean, the distribution of accretionary orogens (Condie, 2007) and UHT terrains (Harley, 1998; Brown & Johnson, 2018) (**Fig. 7b,c**) shows that there is no direct correlation between each supercontinent amalgamation event and heavy carbon isotope markers. In addition, while the abundance of accretionary orogens through Earth history does not change significantly, there are four distinct periods of continental collision flare-ups, 0 - 0.1 Ga; 0.3 - 0.4 Ga; 0.5 - 0.7 Ga and 1.8 - 2.2 Ga (Condie et al., 2007). The continuous presence of accretionary arcs for the past 3000 Ma (which may or may not have resulted from modern plate tectonics processes), might explain why igneous and mafic granulites are more abundant in the geological record (Rudnick & Gao, 2003; Clemens et al., 2020), which introduces some interpretation bias concerning the source carbon in the lower crust. Regarding UHT events, except for Rodinia, every supercontinent (Pangea/Gondwana and Nuna/Columbia) as well as the supercratonic event are charaterised by a decrease in UHT terrains abundance during their assembly phase. It is likely that carbon-bearing fluids found in UHT terrains during the Boring Billion (0.75 - 1.75 Ga – Cawood & Hawkesworth, 2014) is rather the result of double-sided subductions and flat and long-lasting continental orogens (Spencer et al., 2021). In such settings, a significant amount of mantle-derived magma is expected to pond at the crust mantle

interface, potentially helping the delivery of mantle metasomatic fluids into the lower continental crust (Woolley, 1987; Martin, 2006; McLelland & Selleck, 2011). Long-lasting subduction systems resulting in modern-like plate tectonics activity is thought to have occurred between 0 and 0.7 Gyr and 1.6 - 2.1 Ga time, when the coupling between surface and deep Earth mechanisms and crustal reworking were at their highest (Holder et al., 2019; Palin et al., 2020, Sobolev & Brown, 2019; Tang et al., 2021). These periods were predated by an increase in sedimentary discharge in convergent settings (**Fig. 8**) (Bradley, 2008). During these time spans, the carbon isotopic signature in the lower crust has a strong organic component, suggesting intense recycling and reworking of supracrustal materials. It also corresponds to periods of maximum continental collision activity (**Fig. 7b**), the presence of marble and metacarbonates in exhumed lower crustal terrains and an increase in the abundance of S-type granites (**Fig. 8a, b**). From a melt/fluid inclusions perspective, orogenic events in the Phanerozoic also coincide with an increase in abundance of CO$_2$-bearing melt inclusions in high-grade metamorphic minerals, as discussed by Nicoli & Ferrero (2021) (**Fig. 8c**).

Overall, there is abundant evidence pointing toward an internal origin for the lower crustal carbon at specific periods of Earth history. The abundance of mineral phases with a strong organic signature during periods of supercontinentality (Ernst, 2009) in itself suggests that a significant volume of supracrustal carbon was recycled and reworked during continental collision activity. Collection of melt inclusion data on Paleoproterozoic rocks, currently an under-represented period of Earth history (**Fig. 8c**), would help support this hypothesis.

5. Conclusion and perspective

The discovery of inclusions of former anatectic melt in sedimentary granulites (Cesare et al., 2009) provided an important turning point for the study of anatectic processes in the lower crust. These inclusions preserve information about the original composition of the melt and about the volatile budget of the deep continental crust. In situ measurement of the volatile content in the anatectic melt after inclusion rehomogenisation can be used to link orogenic activity to the carbon cycle through the means of crustal thickening and prograde metamorphism. Garnet is a pretty resilient mineral, produced along with the melt phase, which makes it a great time capsule. Despite initial doubts (Clemens, 2009), almost two decades of research in the field of anatectic melt inclusions has shown that the inclusions contained in the garnet represent the perfect “message in the bottle” that can be used when information on the bulk rock are missing (e.g., in heterogeneous migmatite terrains), when liquid has largely escaped, or when mountains have been eroded.

The general source of carbon is still an open question in many granulitic terrains but the two case studies presented here, Ivrea Zone and Central Maine Terrane, shed light on the possible processes which might help understanding the carbon budget of the lower crust in continental collision settings.

Journal Pre-proof

The main findings of our study can be summarised as followed:

1 – Thanks to preserved inclusions in garnet, we were able to constrain the minimum concentration of internally derived bulk rock CO_2 in the partial melted sedimentary lower crust between 400 ppm and 3000 ppm.

2 – As for intermediate and mafic melts, there is a direct positive correlation between silicate melts derived from crustal anatexis and depth. Further experimental work would be required to investigate this relationship in more details (i.e., different protolith and larger range of pressures).

3 –Along with the input from carbonate and organic matter, siliciclastic sediments represent a flux of 5.2 - 9.4 Mt C/yr towards the deep crust during the Phanerozoic. The total flux into the lower continental crust (igneous + sedimentary) is therefore 5.2-56.4 Mt C/yr. This carbon might be ultimately remobilised during volcanic activity on the short term, or, in stable continental crust, by uplift and erosion on the long term.

4 – The compilation of the abundance of melt inclusions and S-type granites at different moments of Earth history, along with isotopic data, orogenic activity, and the distribution of metacarbonate deposits and UHT terrains, collectively points towards periods of intense interaction between the surface and the continental crust. The protracted growth and differentiation of the crust through the reworking of supracrustal materials in continental collision settings is, at specific time of Earth history, a key element of solid carbon storage processes. The stability of the continental crust through time provides one ultimate, long-lasting reservoir of carbon.

5 – The nature of the source of the deep crustal carbon might have changed with time, with periods dominated by internal reworking rather than external inputs.

Finally, the examples used in this contribution only concern the Phanerozoic. Thus, in the future, it is fundamental to tackle Precambrian granulitic terrains in order to better assess the impact of continental collision on the volatile cycle during the early stages of Earth evolution. Recent studies already pointed out the presence of similar melt inclusions in the Neoarchean Basement in Canada (Tacchetto et al., 2018) and in the Mesoarchean Basement in East Greenland (Nicoli et al., 2022b).

The following are the supplementary data related to this article.

Supplementary Table S1 – Measured values of H_2O and CO_2 concentration in rehomogenised melt inclusions

Supplementary Table S2 - Compilation of graphite $\delta^{13}C$ in upper amphibolite facies to UHT rocks.

Acknowledgements

The authors thank Balz Kamber, Jay. J. Ague and Jörg Hermann for their support and constructive comments. SF and AB are grateful to the German Federal Ministry for Education and Research and the Deutsche Forschungsgemeinschaft (Project FE 1527/2-1, FE 1527/2-2, FE 1527/2-3 and FE

Journal Pre-proof

1527/4-1) to S.F. This research was supported through the Alexander von Humboldt Foundation to GN.

References

Acosta-Vigil, A., Barich, A., Bartoli, O., Garrido, C. J., Cesare, B., Remusat, L., ... & Raepsaet, C. (2016). The composition of nanogranitoids in migmatites overlying the Ronda peridotites (Betic Cordillera, S Spain): the anatectic history of a polymetamorphic basement. *Contributions to Mineralogy and Petrology*, *171*(3), 24.

Ague, J. J. (1991). Evidence for major mass transfer and volume strain during regional metamorphism of pelites. *Geology*, *19*(8), 855-858.

Ague, J. J. (2003). Release of CO2 from carbonate rocks during regional metamorphism of lithologically heterogeneous crust. *Geology*, *28*(12), 1123-1126.

Ague, J. J., Eckert Jr, J. O., Chu, X., Baxter, E. F., & Chamberlain, C. P. (2013). Discovery of ultrahigh-temperature metamorphism in the Acadian orogen, Connecticut, USA. *Geology*, *41*(2), 271-274.

Axler, J. A., & Ague, J. J. (2015). Exsolution of rutile or apatite precipitates surrounding ruptured inclusions in garnet from UHT and UHP rocks. *Journal of Metamorphic Geology*, *33*(8), 829-848.

Baiju, K. R., Satish-Kumar, M., Kagi, H., Nambiar, C. G., & Ravisankar, M. (2005). Mineralogical characterization of graphite deposits from Thoduvuzha-Kanjirappally belt, Madurai granulite block, Southern India. Gondwana Research, 8(2), 223-230.

Baker, D. R., & Alletti, M. (2012). Fluid saturation and volatile partitioning between melts and hydrous fluids in crustal magmatic systems: The contribution of experimental measurements and solubility models. *Earth-Science Reviews*, *114*(3-4), 298-324.

Bartoli, O., Cesare, B., Remusat, L., Acosta-Vigil, A., & Poli, S. (2014). The H2O content of granite embryos. *Earth and Planetary Science Letters*, *395*, 281-290.

Bartoli, O., Cesare, B., 2020. Nanorocks: a 10–year–old story. Rendiconti Lincei. Scienze Fisiche e Naturali 31, 249–257.

Bartoli, O. (2021) Characterizing fluid and melt in high-grade metamorphic rocks. In: Lecumberri-Sanchez P, Steele-McInnis M (eds) Fluid inclusions, Mineral Assoc Can, Short Course Ser vol 49.

Berner, R. A., & Caldeira, K. (1997). The need for mass balance and feedback in the geochemical carbon cycle. *Geology*, *25*(10), 955-956.

Berner, R. A., & Kothavala, Z. (2001). GEOCARB III: a revised model of atmospheric CO2 over Phanerozoic time. *American Journal of Science*, *301*(2), 182-204.

Borghini, A., Nicoli, G., Ferrero, S., O'Brien, P. J., Laurent, O., Remusat, L., ... & Milani, S. (2022). *Deep subduction of continental crust contributes to mantle metasomatism and deep carbon cycle* (No. EGU22-5782). Copernicus Meetings.

Bradley, D. C. (2008). Passive margins through earth history. *Earth-Science Reviews*, *91*(1-4), 1-26.

Broekmans, M. A. T. M., Timo G. Nijland, and J. Ben H. Jansen. "Are stable isotopic trends in amphibolite to granulite facies transitions metamorphic or diagenetic?-An answer for the Arendal Area (Bamble Sector, southeastern Norway) from Mid-Proterozoic carbon-bearing rocks." American Journal of Science 294.9 (1994): 1135-1165.

Brown, M. (2006). Duality of thermal regimes is the distinctive characteristic of plate tectonics since the Neoarchean. *Geology*, *34*(11), 961-964.

Brown, M., Kirkland, C. L., & Johnson, T. E. (2020). Evolution of geodynamics since the Archean: Significant change at the dawn of the Phanerozoic. *Geology*, *48*(5), 488-492.

Brown, M., & Johnson, T. (2018). Secular change in metamorphism and the onset of global plate tectonics. *American Mineralogist: Journal of Earth and Planetary Materials*, *103*(2), 181-196.

Brown, M., & Johnson, T. (2019). Time's arrow, time's cycle: Granulite metamorphism and geodynamics. *Mineralogical Magazine*, *83*(3), 323-338.

Bucher-Nurminen, K. (1990). Transfer of mantle fluids to the lower continental crust: Constraints from mantle mineralogy and Moho temperature. *Chemical geology*, *83*(3-4), 249-261.

Carvalho, B. B., Bartoli, O., Cesare, B., Tacchetto, T., Gianola, O., Ferri, F., ... & Szabó, C. (2020). Primary CO2-bearing fluid inclusions in granulitic garnet usually do not survive. *Earth and Planetary Science Letters*, *536*, 116170.

Carvalho, B. B., Bartoli, O., Ferri, F., Cesare, B., Ferrero, S., Remusat, L., ... & Poli, S. (2019). Anatexis and fluid regime of the deep continental crust: New clues from melt and fluid inclusions in metapelitic migmatites from Ivrea Zone (NW Italy). *Journal of Metamorphic Geology*, *37*(7), 951-975.

Catling, D. C. & Zahnle, K. J. (2020). The Archean Atmosphere. *Science Advances*, *6 (9).*

Cawood, P. A., & Hawkesworth, C. J. (2014). Earth's middle age. *Geology*, *42*(6), 503-506.

Cesare, B., Maineri, C., Toaldo, A. B., Pedron, D., & Vigil, A. A. (2007). Immiscibility between carbonic fluids and granitic melts during crustal anatexis: a fluid and melt inclusion study in the enclaves of the Neogene Volcanic Province of SE Spain. *Chemical Geology*, *237*(3-4), 433-449.

Cesare, B., Meli, S., Nodari, L., & Russo, U. (2005). Fe 3+ reduction during biotite melting in graphitic metapelites: anotner origin of CO_2 in granulites. *Contributions to Mineralogy and Petrology*, *149*(2), 129-140.

Cesare, B. (2008) Crustal melting: Working with enclaves. In E.W. Sawyer and M. Brown, Eds., Working with Migmatites, 37–55. Mineralogical Association of Canada, Short Course 38, Quebec City

Cesare, B., Ferrero, S., Salvioli-Mariani, E., Pedron, D., and Cavallo, A. (2009) Nanogranite and glassy inclusions: the anatectic melt in migmatites and granulites. Geology, 37, 627–630.

Chu, X., & Ague, J. J. (2013). Phase equilibria for graphitic metapelite including solution of CO 2 in melt and cordierite: implications for dehydration, partial melting and graphite precipitation. *Journal of Metamorphic Geology*, *31*(8), 843-862.

Journal Pre-proof

Clemens, J. D. (1990). The granulite—granite connexion. In *Granulites and crustal evolution* (pp. 25-36). Springer, Dordrecht.

Clemens, J. D. (2006). *Melting of the continental crust: fluid regimes, melting reactions, and source-rock fertility* (pp. 297-331). Cambridge University Press.

Clemens, J.D. (2009). The message in the bottle: "melt" inclusions in migmatitic garnets. *Geology, 37,* 671–672.

Clemens, J. D., Buick, I. S., & Stevens, G. (2016). Fluids, melting, granulites and granites: A controversy–reply to the commentary of. *Precambrian Research*, *278*, 400-404.

Clemens, J. D., Droop, G. T., & Stevens, G. (1997). High-grade metamorphism, dehydration and crustal melting: a reinvestigation based on new experiments in the silica-saturated portion of the system KAlO 2–MgO–SiO 2–H 2 O–CO 2 at P≤ 1.5 GPa. *Contributions to Mineralogy and Petrology*, *129*(4), 308-325.

Clemens, J. D., Stevens, G., & Bryan, S. E. (2020). Conditions during the formation of granitic magmas by crustal melting–hot or cold; drenched, damp or dry?. *Earth-Science Reviews*, *200*, 102982.

Clemens, J., & Watkins, J. M. (2001). The fluid regime of high-temperature metamorphism during granitoid magma genesis. *Contributions to Mineralogy and Petrology*, *140*(5), 600-606.

Collerson, K. D., & Fryer, B. J. (1978). The role of fluids in the formation and subsequent development of early continental crust. *Contributions to Mineralogy and Petrology*, *67*(2), 151-167.

Condie, K. C. (1993). Chemical composition and evolution of the upper continental crust: contrasting results from surface samples and shales. *Chemical geology*, *104*(1-4), 1-37.

Condie, K. C., Hatcher, R. D., Carlson, M. P., & McBride, J. H. (2007). Accretionary orogens in space and time. *Memoir-Geological Society of America*, *200*, 145.

Condie, K. C., Arndt, N., Davaille, A., & Puetz, S. J. (2017). Zircon age peaks: Production or preservation of continental crust?. *Geosphere*, *13*(2), 227-234.

Dhuime, B., Wuestefeld, A., & Hawkesworth, C. J. (2015). Emergence of modern continental crust about 3 billion years ago. *Nature Geoscience*, *8*(7), 552-555.

Dobrzhinetskaya, L. F., Green, H. W., Takahata, N., Sano, Y., & Shirai, K. (2010). Crustal signature of δ 13 C and nitrogen content in microdiamonds from Erzgebirge, Germany: Ion microprobe studies. *Journal of Earth Science*, *21*(5), 623-634.

Dunai, T. J., & Touret, J. L. R. (1993). A noble gas study of a granulite sample from the Nilgiri Hills, southern India: implications for granulite formation. *Earth and Planetary Science Letters*, *119*(3), 271-281.

Ernst, W. G. (2009). Archean plate tectonics, rise of Proterozoic supercontinentality and onset of regional, episodic stagnant-lid behavior. *Gondwana Research*, *15*(3-4), 243-253.

Ferrero, S., Ague, J. J., O'Brien, P. J., Wunder, B., Remusat, L., Ziemann, M. A., & Axler, J. (2021a). High-pressure, halogen-bearing melt preserved in ultrahigh-temperature felsic granulites of the

Central Maine Terrane, Connecticut (USA). *American Mineralogist: Journal of Earth and Planetary Materials*, *106*(8), 1225-1236.

Ferrero, S., Wannhoff, I., Laurent, O., Yakymchuk, C., Darling, R., Wunder, B., ... & O'Brien, P. J. (2021b). Embryos of TTGs in Gore Mountain garnet megacrysts from water-fluxed melting of the lower crust. *Earth and Planetary Science Letters*, *569*, 117058.

Ferri, F., Cesare, B., Bartoli, O., Ferrero, S., Palmeri, R., Remusat, L., & Poli, S. (2020). Melt inclusions at MT. Edixon (Antarctica): Chemistry, petrology and implications for the evolution of the Lanterman range. *Lithos*, *374*, 105685.

Ferry, J. M. (1988). Infiltration-driven metamorphism in northern New England, USA. *Journal of Petrology*, *29*(6), 1121-1159.

Fitzsimons, I.C.W., Clark, C., Chilekwa, M. & Santosh, M. (2018). The dark history of charnockite. Granulites and granulites, Ullapool, Scotland.

Foley, B. J. (2015). The role of plate tectonic–climate coupling and exposed land area in the development of habitable climates on rocky planets. *The Astrophysical Journal*, *812*(1), 36.

Gaillardet, J., Dupré, B., Louvat, P., & Allegre, C. J. (1999). Global silicate weathering and CO2 consumption rates deduced from the chemistry of large rivers. *Chemical geology*, *159*(1-4), 3-30.

Gerya, T., Stern, R., Pellissier, L., & Stemmler, D. (2020). Bio-geodynamics of the Earth: State of the art and future directions. *EGU2020*, (EGU2020-10657).

Gianola, O., Bartoli, O., Ferri, F., Galli, A., Ferrero, S., Capizzi, L. S., ... & Cesare, B. (2021). Anatectic melt inclusions in ultra high temperature granulites. *Journal of Metamorphic Geology*, *39*(3), 321-342.

Gianola, O., Costa, B., Alvaro, M., Gilio, M., Ferri, F., & Cesare, B. (2022) Origin of felsic melts by anatexis of arclogites in arc roots: an example from Mercaderes, Colombia. MSG RIP 2022, St Andrews, Scotland.

Glassley, W. E. (1983). The role of CO2 in the chemical modification of deep continental crust. *Geochimica et Cosmochimica Acta*, *47*(3), 597-616.

Glover, P. W. J. (1996). Graphite and electrical conductivity in the lower continental crust: a review. *Physics and Chemistry of the Earth*, *21*(4), 279-287.

Guo, M., & Korenaga, J. (2020). Argon constraints on the early growth of felsic continental crust. *Science advances*, *6*(21), eaaz6234.

Harley, S. L. (1989). The origins of granulites: a metamorphic perspective. *Geological Magazine*, *126*(3), 215-247.

Harley, S. L. (1998). On the occurrence and characterization of ultrahigh-temperature crustal metamorphism. *Geological Society, London, Special Publications*, *138*(1), 81-107.

Hawkesworth, C. J., & Brown, M. (2018). Earth dynamics and the development of plate tectonics. *Philosophical Transactions of the Royal Society A: Mathematical, Physical and Engineering Sciences*, *376*(2132), 20180228.

Journal Pre-proof

Hawkesworth, C., & Jaupart, C. (2021). Heat flow constraints on the mafic character of Archean continental crust. *Earth and Planetary Science Letters*, *571*, 117091.

Hoernes, S., Fiorentini, E., & Hoffbauer, R. (1994). The role of fluids in granulite-facies metamorphism as deduced from oxygen and carbon isotopic compositions. Precambrian research, 66(1-4), 183-198.

Hoffbauer, R., & Spiering, B. (1994). Petrologic phase equilibria and stable isotope fractionations of carbonate-silicate parageneses from granulite-grade rocks of Sri Lanka. Precambrian research, 66(1-4), 325-349.

Holder, R. M., Viete, D. R., Brown, M., & Johnson, T. E. (2019). Metamorphism and the evolution of plate tectonics. *Nature*, *572*(7769), 378-381.

Hollister, L. S. (1988). On the origin of CO2-rich fluid inclusions in migmatites. *Journal of Metamorphic Geology*, *6*(4), 467-474.

Holloway, J. R. (1976). Fluids in the evolution of granitic magmas: consequences of finite CO2 solubility. *Geological Society of America Bulletin*, *87*(10), 1513-1518.

Holtz, F., Behrens, H., Dingwell, D. B., & Johannes, W. (1995). H2O solubility in haplogranitic melts: compositional, pressure, and temperature dependence. *American Mineralogist*, *80*(1-2), 94-108.

Huizenga, J. M., & Touret, J. L. (2012). Granulites, CO2 and graphite. *Gondwana Research*, *22*(3-4), 799-809.

Jackson, D. H., Mattey, D. P., & Harris, N. B. W. (1988). Carbon isotope compositions of fluid inclusions in charnockites from southern India. *Nature*, *333*(6169), 167-170.

Kelemen, P. B., & Manning, C. E. (2015). Reevaluating carbon fluxes in subduction zones, what goes down, mostly comes up. *Proceedings of the National Academy of Sciences*, *112*(30), E3997-E4006.

Kempton, P. D., Harmon, R. S., Hawkesworth, C. J., & Moorbath, S. (1990). Petrology and geochemistry of lower crustal granulites from the Geronimo Volcanic Field, southeastern Arizona. *Geochimica et Cosmochimica Acta*, *54*(12), 3401-3426.

Kerrick, D. M., & Connolly, J. A. D. (2001). Metamorphic devolatilization of subducted oceanic metabasalts: implications for seismicity, arc magmatism and volatile recycling. *Earth and Planetary Science Letters*, *189*(1-2), 19-29.

Korenaga, J. (2018). Crustal evolution and mantle dynamics through Earth history. *Philosophical Transactions of the Royal Society A: Mathematical, Physical and Engineering Sciences*, *376*(2132), 20170408.

Korenaga, J., Planavsky, N. J., & Evans, D. A. (2017). Global water cycle and the coevolution of the Earth's interior and surface environment. *Philosophical Transactions of the Royal Society A: Mathematical, Physical and Engineering Sciences*, *375*(2094), 20150393.

Kramers, J. D., & Tolstikhin, I. N. (1997). Two terrestrial lead isotope paradoxes, forward transport modelling, core formation and the history of the continental crust. *Chemical geology*, *139*(1-4), 75-110.

Journal Pre-proof

Kretz, R. (1983). Symbols for rock-forming minerals. *American mineralogist*, *68*(1-2), 277-279.

Lamadrid, H. M., & Steele-MacInnis, M. (2021). Crustal melting: Deep, hot, and salty. *American Mineralogist*, *106*(8), 1193-1194.

Lyubetskaya, T., & Ague, J. J. (2009). Modeling the magnitudes and directions of regional metamorphic fluid flow in collisional orogens. *Journal of Petrology*, *50*(8), 1505-1531.

McCulloch, M. T. (1993). The role of subducted slabs in an evolving earth. *Earth and Planetary Science Letters*, *115*(1-4), 89-100.

Miranda, D. A., de Oliveira Chaves, A., Campello, M. S., & Ramos, S. L. L. D. M. (2019). Origin and thermometry of graphites from Itapecerica supracrustal succession of the southern Sao Francisco Craton by C isotopes, X-ray diffraction, and Raman spectroscopy. International Geology Review, 61(15), 1864-1875.

Newton, R. C., Smith, J. V., & Windley, B. F. (1980). Carbonic metamorphism, granulites and crustal growth. *Nature*, *288*(5786), 45-50.

Newton, R. C., Touret, J. L., & Aranovich, L. Y. (2014). Fluids and H2O activity at the onset of granulite facies metamorphism. *Precambrian Research*, *253*, 17-25.

Nicoli, G., & Dyck, B. (2018). Exploring the metamorphic consequences of secular change in the siliciclastic compositions of continental margins. *Geoscience Frontiers*, *9*(4), 967-975.

Nicoli, G., Ferrero, S., Darling, R., Yakymchuk, C., Wunder, B., & Tollan, P. (2022a). *Multiple partial melts trapped in garnets from the Adirondacks lower crust: clues for TTG formation* (No. EGU22-2271). Copernicus Meetings.

Nicoli, G., Gresky, K., & Ferrero, S. (2022b). Mesoarchean melt and fluid inclusions in garnet from the Kangerlussuaq basement, Southeast Greenland. *Mineralogia*, *53*.

Nicoli, G., & Ferrero, S. (2021). Nanorocks, volatiles and plate tectonics. *Geoscience Frontiers*, *12*(5), 101188.

Nicoli, G., Stevens, G., Moyen, J. F., Vezinet, A., & Mayne, M. (2017). Insights into the complexity of crustal differentiation: K2O-poor leucosomes within metasedimentary migmatites from the Southern Marginal Zone of the Limpopo Belt, South Africa. *Journal of Metamorphic Geology*, *35*(9), 999-1022.

Okudaira, T., Shigematsu, N., Harigane, Y., & Yoshida, K. (2017). Grain size reduction due to fracturing and subsequent grain-size-sensitive creep in a lower crustal shear zone in the presence of a CO2-bearing fluid. *Journal of Structural Geology*, *95*, 171-187.

Palin, R. M., Santosh, M., Cao, W., Li, S. S., Hernández-Uribe, D., & Parsons, A. (2020). Secular change and the onset of plate tectonics on Earth. *Earth-Science Reviews*, *207*, 103172.

Parnell, J., Brolly, C., & Boyce, A. (2021). Mixed metamorphic and fluid graphite deposition in Palaeoproterozoic supracrustal rocks of the Lewisian Complex, NW Scotland. Terra Nova.

Peck, W. H. (2016). Protolith carbon isotope ratios in cordierite from metamorphic and igneous rocks. *American Mineralogist*, *101*(10), 2279-2287.

Journal Pre-proof

Peterson, J. W., & Newton, R. C. (1989). CO2-enhanced melting of biotite-bearing rocks at deep-crustal pressure–temperature conditions. *Nature*, *340*(6232), 378-380.

Pettijohn, F. J. (1963). *Chemical composition of sandstones, excluding carbonate and volcanic sands: Representative analyses* (No. 440). US Government Printing Office.

Quick, J. E., Sinigoi, S., Peressini, G., Demarchi, G., Wooden, J. L., & Sbisà, A. (2009). Magmatic plumbing of a large Permian caldera exposed to a depth of 25 km. *Geology*, *37*(7), 603-606.

Safonov, O. G., Reutsky, V. N., Varlamov, D. A., Yapaskurt, V. O., Golunova, M. A., Shcherbakov, V. D., ... & Butvina, V. G. (2018). Composition and source of fluids in high-temperature graphite-bearing granitoids associated with granulites: Examples from the Southern Marginal Zone, Limpopo Complex, South Africa. Gondwana Research, 60, 129-152.

Sanyal, P., Acharya, B. C., Bhattacharya, S. K., Sarkar, A., Agrawal, S., & Bera, M. K. (2009). Origin of graphite, and temperature of metamorphism in Precambrian Eastern Ghats Mobile Belt, Orissa, India: A carbon isotope approach. Journal of Asian Earth Sciences, 36(2-3), 252-260.

Santosh, M., & Omori, S. (2008). CO2 flushing: a plate tectonic perspective. *Gondwana Research*, *13*(1), 86-102.

Santosh, M., & Wada, H. (1993). Microscale isotopic zonation in graphite crystals: Evidence for channelled CO influx in granulites. Earth and Planetary Science Letters, 119(1-2), 19-26.

Satish-Kumar, M. (2005). Graphite-bearing CO2 fluid inclusions in granulites: Insights on graphite precipitation and carbon isotope evolution. Geochimica et Cosmochimica Acta, 69(15), 3841-3856.

Satish-Kumar, M. (2000). Ultrahigh-temperature metamorphism in Madurai granulites, Southern India: Evidence from carbon isotope thermometry. The Journal of geology, 108(4), 479-486.

Sawyer, E. W. (2010). Migmatites formed by water-fluxed partial melting of a leucogranodiorite protolith: Microstructures in the residual rocks and source of the fluid. *Lithos*, *116*(3-4), 273-286.

Schmid, S. M. (1993). Ivrea zone and adjacent southern Alpine basement. In *Pre-Mesozoic geology in the Alps* (pp. 567-583). Springer, Berlin, Heidelberg.

Schmid, R., & Wood, B. J. (1976). Phase relationships in granulitic metapelites from the Ivrea-Verbano Zone (Northern Italy). *Contributions to Mineralogy and Petrology*, *54*(4), 255-279.

Silver, P. G., & Behn, M. D. (2008). Intermittent plate tectonics?. *science*, *319*(5859), 85-88.

Sobolev, S. V., & Brown, M. (2019). Surface erosion events controlled the evolution of plate tectonics on Earth. *Nature*, *570*(7759), 52-57.

Solomatova, N., Caracas, R., & Cohen, R. (2020). Carbon speciation and solubility in silicate melts. *Carbon in Earth's Interior*, 179-194.

Spencer, C. J., Mitchell, R. N., & Brown, M. (2021). Enigmatic Mid-Proterozoic Orogens: Hot, Thin, and Low. *Geophysical Research Letters*, *48*(16), e2021GL093312.

Stähle, H. J., Raith, M., Hoernes, S., & Delfs, A. (1987). Element mobility during incipient granulite formation at Kabbaldurga, southern India. *Journal of Petrology*, *28*(5), 803-834.

Journal Pre-proof

Stepanov, A. S. (2021). A review of the geochemical changes occurring during metamorphic devolatilization of metasedimentary rocks. *Chemical Geology*, 120080.

Stewart, E. M., & Ague, J. J. (2018). Infiltration-driven metamorphism, New England, USA: Regional CO2 fluxes and implications for Devonian climate and extinctions. *Earth and Planetary Science Letters*, *489*, 123-134.

Tang, M., Chu, X., Hao, J., & Shen, B. (2021). Orogenic quiescence in Earth's middle age. *Science*, *371*(6530), 728-731.

Thompson, A. B., & Tracy, R. J. (1979). Model systems for anatexis of pelitic rocks. *Contributions to Mineralogy and Petrology*, *70*(4), 429-438.

Tian, M., & Ague, J. J. (2014). The impact of porosity waves on crustal reaction progress and CO2 mass transfer. *Earth and Planetary Science Letters*, *390*, 80-92.

Tian, M., Ague, J. J., Chu, X., Baxter, E. F., Dragovic, N., Chamberlain, C. P., & Rumble III, D. (2018). The potential for metamorphic thermal pulses to develop during compaction-driven fluid flow. *Geochemistry, Geophysics, Geosystems*, *19*(1), 232-256.

Touret, J. (1971). Le facies granulite en Norvege Meridionale: II. Les inclusions fluides. *Lithos*, *4*(4), 423-436.

Touret, J. L. (1992). CO2 transfer between the upper mantle and the atmosphere: temporary storage in the lower continental crust. *Terra Nova*, *4*(1), 87-98.

Touret, J. L., & Huizenga, J. M. (2011). Fluids in granulites. *Geological Society of America Memoirs*, *207*, 25-37.

Touret, J. L., & Huizenga, J. M. (2012). Fluid-assisted granulite metamorphism: a continental journey. *Gondwana Research*, *21*(1), 224-235.

Touret, J. L. R., & Huizenga, J. M. (2020). Large-scale fluid transfer between mantle and crust during supercontinent amalgamation and disruption. *Russian Geology and Geophysics*, *61*(5-6), 527-542.

Touret, J. L. R., Santosh, M., & Huizenga, J. M. (2016). High-temperature granulites and supercontinents. *Geoscience Frontiers*, *7*(1), 101-113.

Vielzeuf, D., & Montel, J. M. (1994). Partial melting of metagreywackes. Part I. Fluid-absent experiments and phase relationships. *Contributions to Mineralogy and Petrology*, *117*(4), 375-393.

Vry, J. K., Brown, P. E., & Valley, J. W. (1990). Cordierite volatile content and the role of CO2 in high-grade metamorphism. *American Mineralogist*, *75*(1-2), 71-88.

Wedepohl, K. H. (1995). The composition of the continental crust. *Geochimica et cosmochimica Acta*, *59*(7), 1217-1232.

Weinberg, R. F., & Hasalová, P. (2015). Water-fluxed melting of the continental crust: A review. *Lithos*, *212*, 158-188.

Wong, K., Mason, E., Brune, S., East, M., Edmonds, M., & Zahirovic, S. (2019). Deep carbon cycling over the past 200 million years: a review of fluxes in different tectonic settings. *Frontiers in Earth Science*, *7*, 263.

Journal Pre-proof

Wyllie, P. J. (1977). Effects of H2O and CO2 on magma generation in the crust and mantle. *Journal of the Geological Society*, *134*(2), 215-234.
Yoshioka, T., Nakashima, D., Nakamura, T., Shcheka, S., & Keppler, H. (2019). Carbon solubility in silicate melts in equilibrium with a CO-CO2 gas phase and graphite. *Geochimica et Cosmochimica Acta*, *259*, 129-143.

Figure 1 – (a) Melt inclusions of metasedimentary affinity (Nicoli & Ferrero, 2021). Melt inclusions modelled in this study: Ivrea Zone (IZ) and Central Maine Terrane (CMT). LG – low grade sediments; GS – green schists; Amph – amphibolite; Gn – granulite (including migmatites); B – blue schists; E-HP – high pressure eclogite and UHP – ultra high pressure. Dia-Gr – diamond/graphite boundary; Coe-Qtz – coesite/quartz boundary. Barrovian geotherms: 350-750 °C.GPa-1 (Brown, 2006)

Figure 2 – Garnets with carbon-bearing melt inclusions. (a-c) Ivrea Zone (Italy). (a) Transition zone. (b) Granulite zone (Carvalho et al., 2019). The dashed line delimits the area where inclusions occur. (c) Cluster of nanogranitoids (white arrow) and fluid inclusions (black arrow) in the Ivrea Zone garnet. Modified after Carvalho et al., (2020) (d-f) Central Maine Terrane (Connecticut – US). (d) Transmitted light photomicrograph with main mineral assemblage. (e) Crossed-polars light photomicrograph with the different type of inclusions (Axler & Ague, 2015). Graphite is also found in inclusions but too small to show in here (f) Cluster of needle-shaped nanogranitoids (grey arrow), isometric nanogranitoids (white arrow) and thin rutile needles (red arrow). Modified after Ferrero et al., (2021a). Abbreviations after Kretz (1983).

Figure 3 - Modelled melt CO_2 and H_2O content for different amount of bulk H_2O (wt.%) and bulk CO_2 (isoline – ppm) during prograde metamorphism and decompression. (a) Ivrea Zone. Upper amphibolite zone: white circle; transition zone: grey circle; granulite zone: black circle. Dashed box: average ± 1σ measured composition. The shaded zone indicates the melt is in equilibrium with a COH-fluid. (b) Central Maine Terrane. Pressure and temperature for the start of the P-T path, peak metamorphic conditions and isothermal decompression are reported.

Figure 4 – Modelled melt major element composition for different amount of bulk H_2O along the same P-T paths on Figure 3 (a) Ivrea Zone (see Figure 3 for caption). (b) Central Maine Terrane. ASI (molar Al/[Ca+Na+K]) vs AI (molar Al – [Na+K]); Ca/(Ca+Na) molar ratio vs. SiO_2 (wt.%) and Mg# (molar Mg/[Mg+FeOT]) vs. SiO_2 (wt.%). Dashed box: average ± 1σ measured composition.

Figure 5 –Box plot diagram showing the bulk rock CO_2 content of siliciclastic sediments, their metamorphic equivalent, S-type granites and melt inclusions. The white circle in each box represents

Journal Pre-proof

the average value. Data from http://portal.earthchem.org/. Modelled internally derived bulk CO_2 is shown for comparison.

Figure 6 - Schematic representation of the carbon cycle and long-term storage associated with continental collision. Orogenic burial, solid storage and melt extraction values are from this study whereas the values for outgassing is after Stewart et al. (2019) and the solid storage in the upper mantle is after Kelemen & Manning (2015).

Figure 7 – (a) Carbon isotopic signature of the lower crust. Circle: graphite; black diamond: fluid inclusions; square: cordierite; boxplot: diamond. Supercontinent cycles – P/G: Pangea/Gondwana; R: Rodinia; N/C: Nuna/Columbia. Supercraton: Scr. Assembly and breakup phase after Brown & Johnson (2018). (b) Abundance of collisional and accretionary orogens (Condie et al., 2007). (c) UHT terrains (T > 900 °C) abundance after Brown & Johnson (2019).

Figure 8 – (a) Marbles and metacarbonates abundance in exhumed granulitic terrain. (b) Occurrence of S-type zircons reconstructed from zircons collected in river sediments (modified after Zhu et al., 2020). (c) Main occurrence of inclusions in high-grade metamorphic mineral in different protoliths (Modified after Nicoli & Ferrero, 2021). IZ: Ivrea Zone, CMT: Central Maine Terrane. Terrain with inferred anatectic CO_2 of metasedimentary affinity: A: Athabasca (Tacchetto et al. 2019); UP: Uttental Plateau (Nicoli et al., 2022b). The vertical pink bands correspond to period of enhanced sedimentary discharge in convergent settings (Sobolev & Brown, 2019).
Continental crust after Tang et al. (2021) and frequency of orogens after Condie et al. (2017.

Table 1 -Starting material composition (in wt.%). Shale composition are from Ague (1991) whereas the greywacke composition is from Pettijohn (1963). Mg# = Mg/[Mg+Fe_T]; A/CNK = Al/[Ca+Na+K]; Ca# = Ca/[Ca+Na].

	Shale	Greywacke
SiO2	63.56	71.29
TiO2	0.80	0.77
Al2O3	17.96	12.48
Fe2O3	0.93	0.59
FeO	6.83	4.33
MgO	2.83	3.06
MnO	0.09	0.05
CaO	1.53	0.52
Na2O	1.63	5.04
K2O	3.83	1.87
Mg#	0.40	0.53
A/CNK	2.18	1.16
Ca#	0.34	0.05

Journal Pre-proof

Journal Pre-proof

Declaration of interests

The authors declare that they have no known competing financial interests or personal relationships that could have appeared to influence the work reported in this paper.

The authors declare the following financial interests/personal relationships which may be considered as potential competing interests

Journal Pre-proof

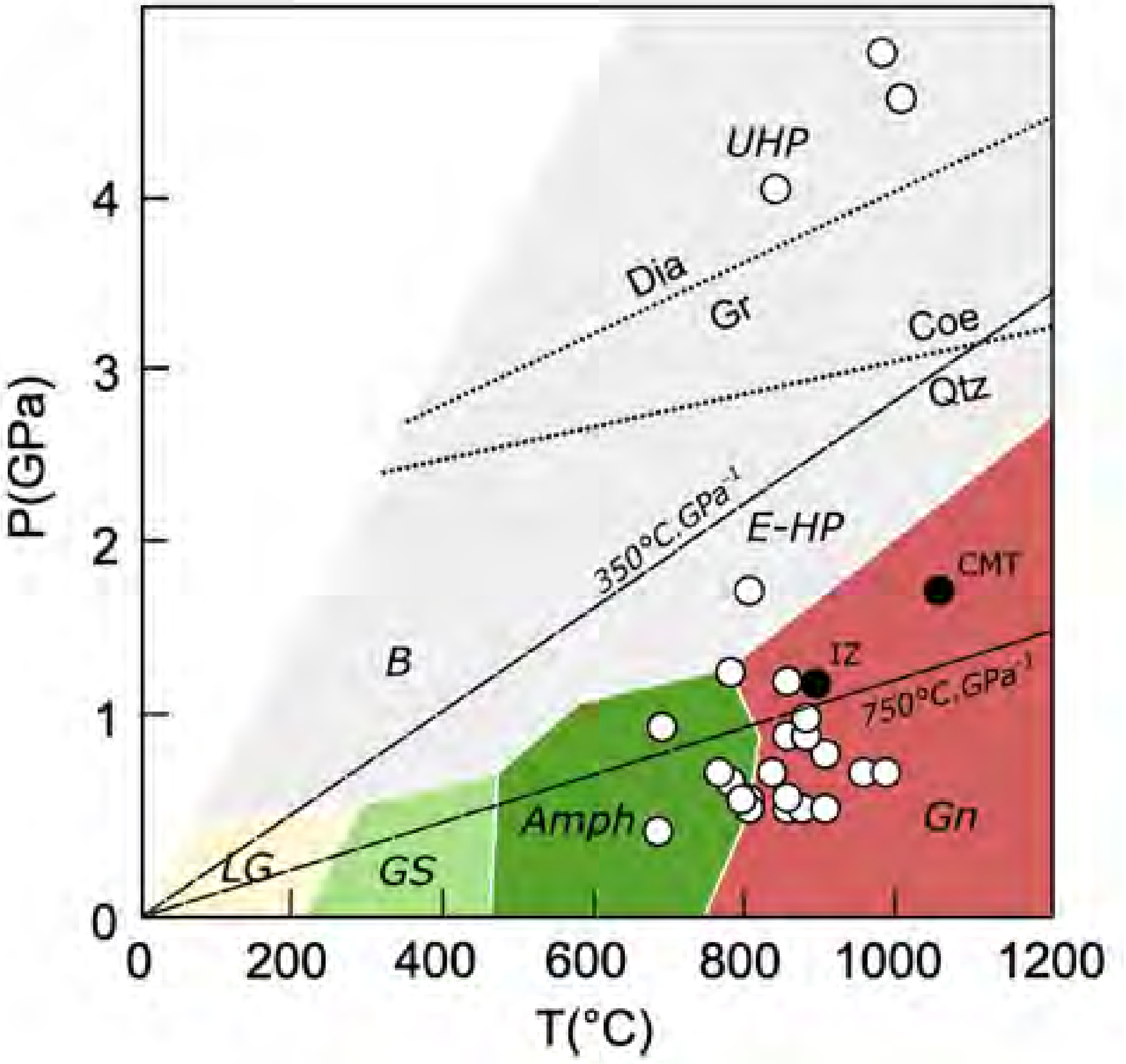
P(GPa)
T(°C)
0
1
2
3
4
0
200
400
600
800
1000
1200
UHP
Dia
Gr
Coe
Qtz
350°C.GPa⁻¹
E-HP
CMT
IZ
B
750°C.GPa⁻¹
Amph
Gn
LG
GS

Figure 1

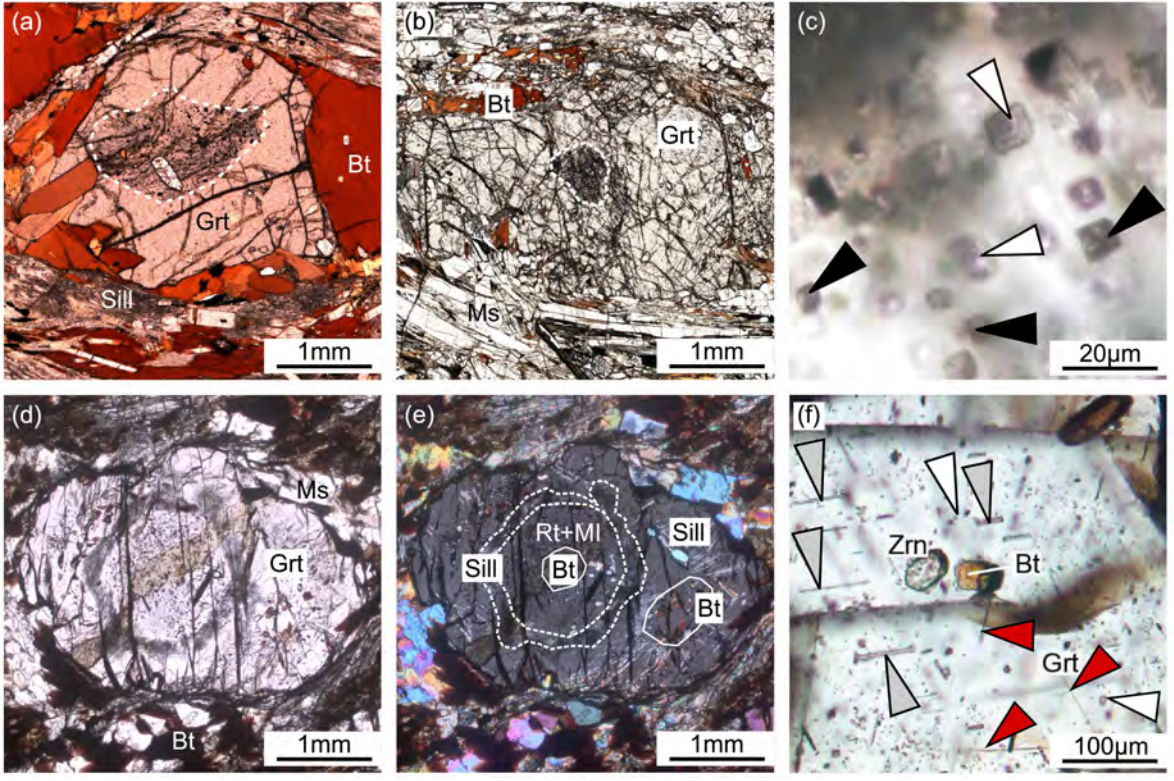
(a)
Bt
Grt
Sill
1mm
(b)
Bt
Grt
Ms
1mm
(c)
20μm
(d)
Ms
Grt
Bt
1mm
(e)
Rt+Ml
Sill
Sill
Bt
Bt
1mm
(f)
Zrn
Bt
Grt
100μm

Figure 2

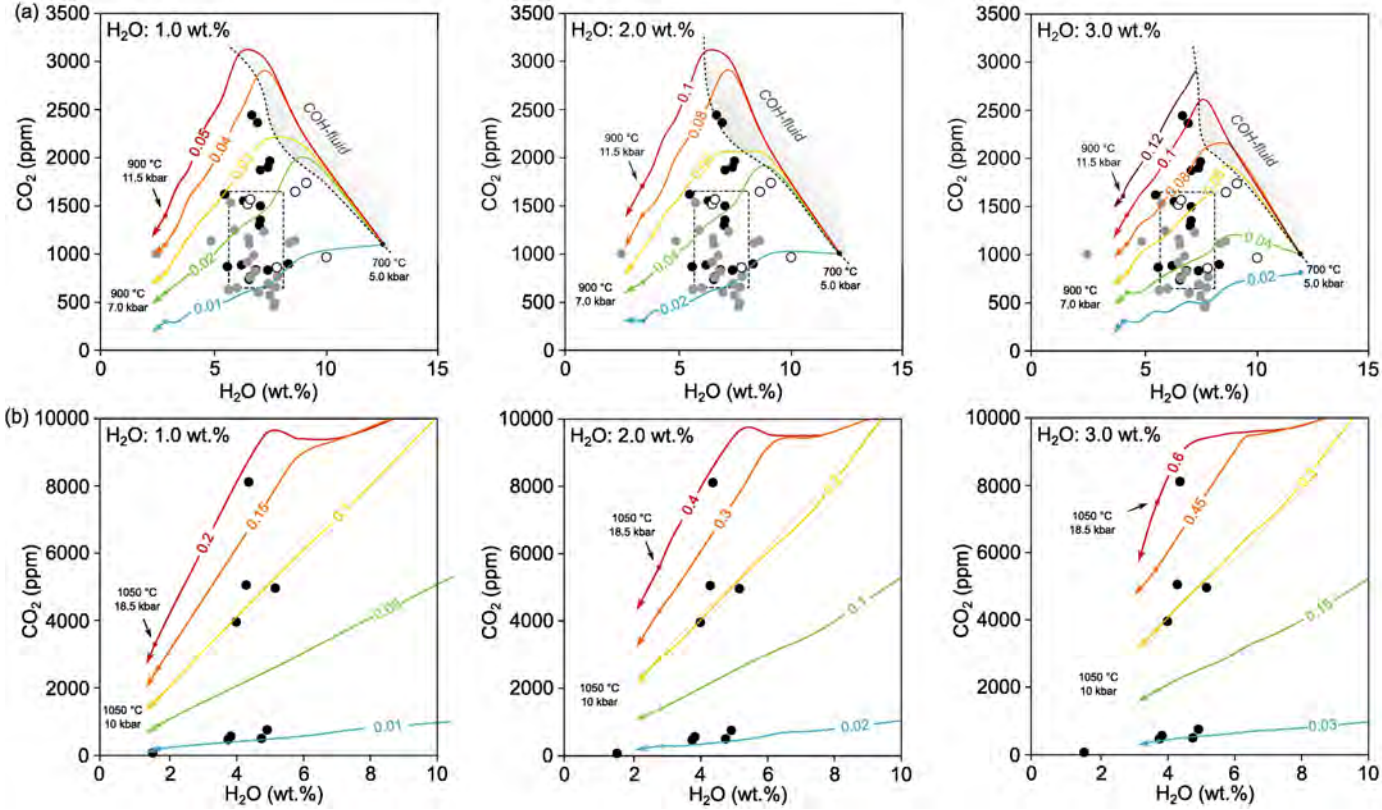
(a)
H2O: 1.0 wt.%
H2O: 2.0 wt.%
H2O: 3.0 wt.%
CO2 (ppm)
H2O (wt.%)
COH-fluid
900 °C
11.5 kbar
900 °C
7.0 kbar
700 °C
5.0 kbar
0.05
0.04
0.03
0.02
0.01
0.1
0.09
0.08
0.07
0.06
0.12
(b)
1050 °C
18.5 kbar
1050 °C
10 kbar
0.2
0.15
0.1
0.09
0.4
0.3
0.6
0.45

Figure 3

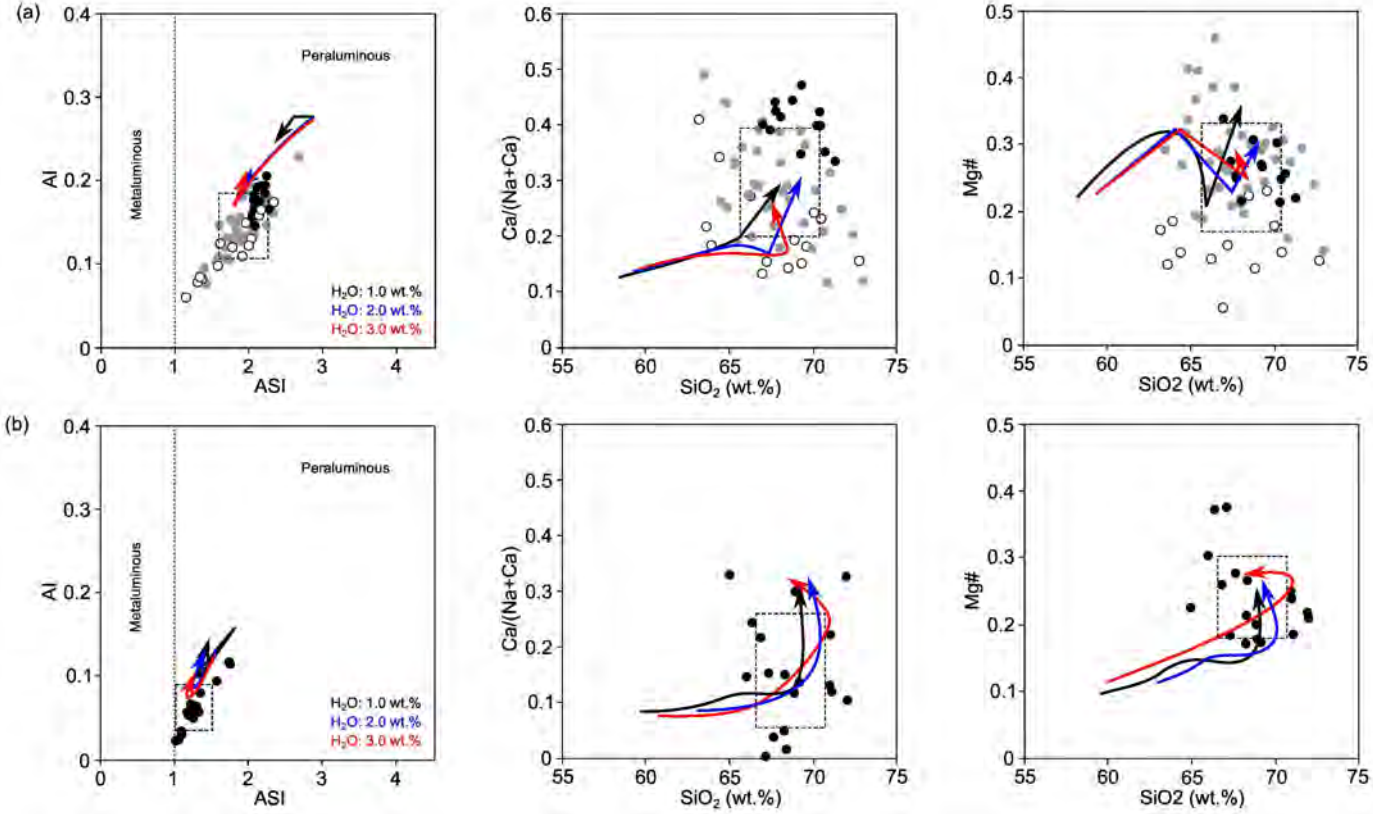
(a)
Peraluminous
Metaluminous
AI
ASI
H2O: 1.0 wt.%
H2O: 2.0 wt.%
H2O: 3.0 wt.%
Ca/(Na+Ca)
SiO2 (wt.%)
Mg#
SiO2 (wt.%)
(b)
Peraluminous
Metaluminous
AI
ASI
H2O: 1.0 wt.%
H2O: 2.0 wt.%
H2O: 3.0 wt.%
Ca/(Na+Ca)
SiO2 (wt.%)
Mg#
SiO2 (wt.%)

Figure 4

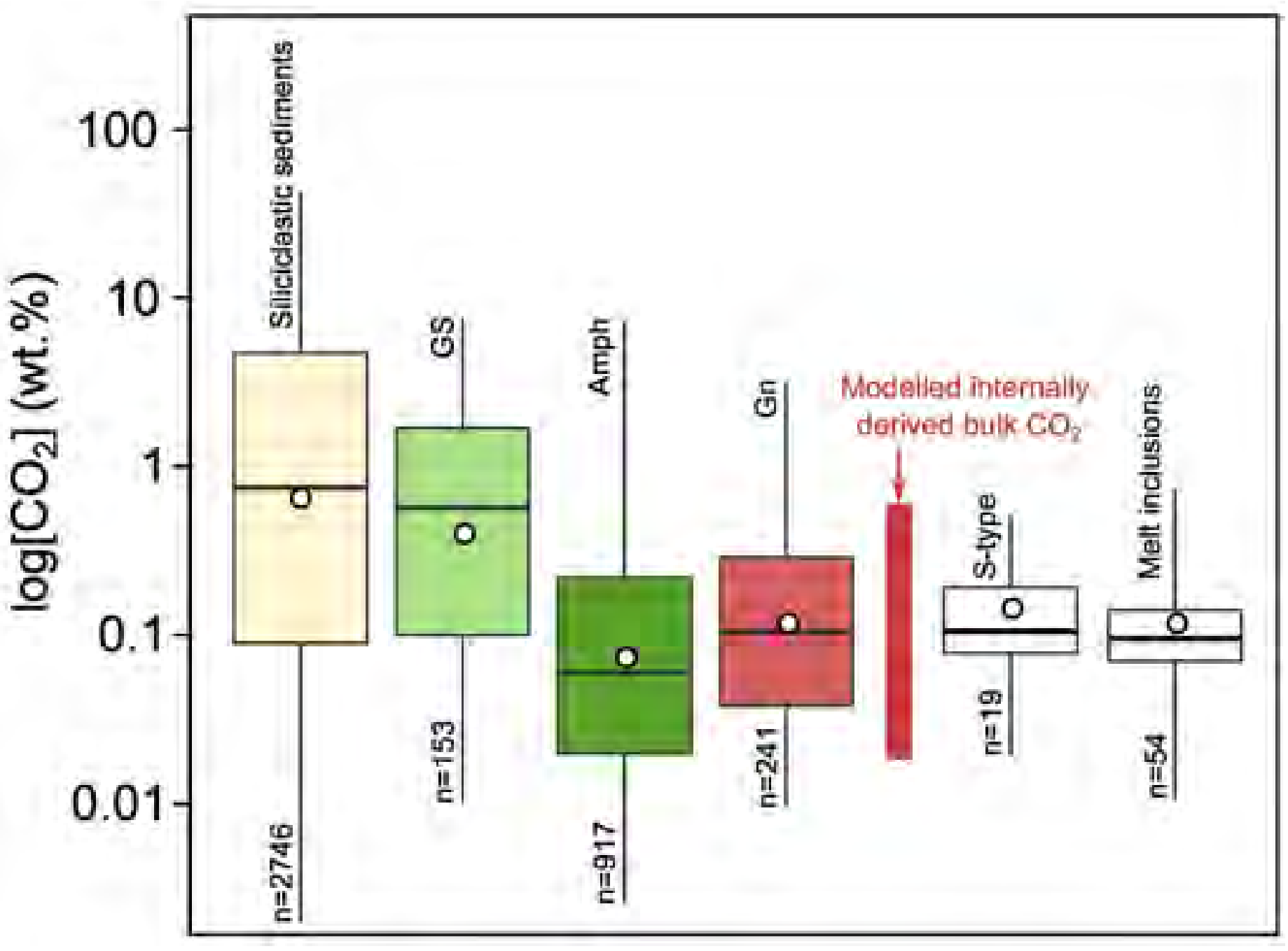
log[CO2] (wt.%)
100
10
1
0.1
0.01
Siliciclastic sediments
n=2746
GS
n=153
Amph
n=917
Gn
n=241
Modelled internally derived bulk CO2
S-type
n=19
Melt inclusions
n=54

Figure 5

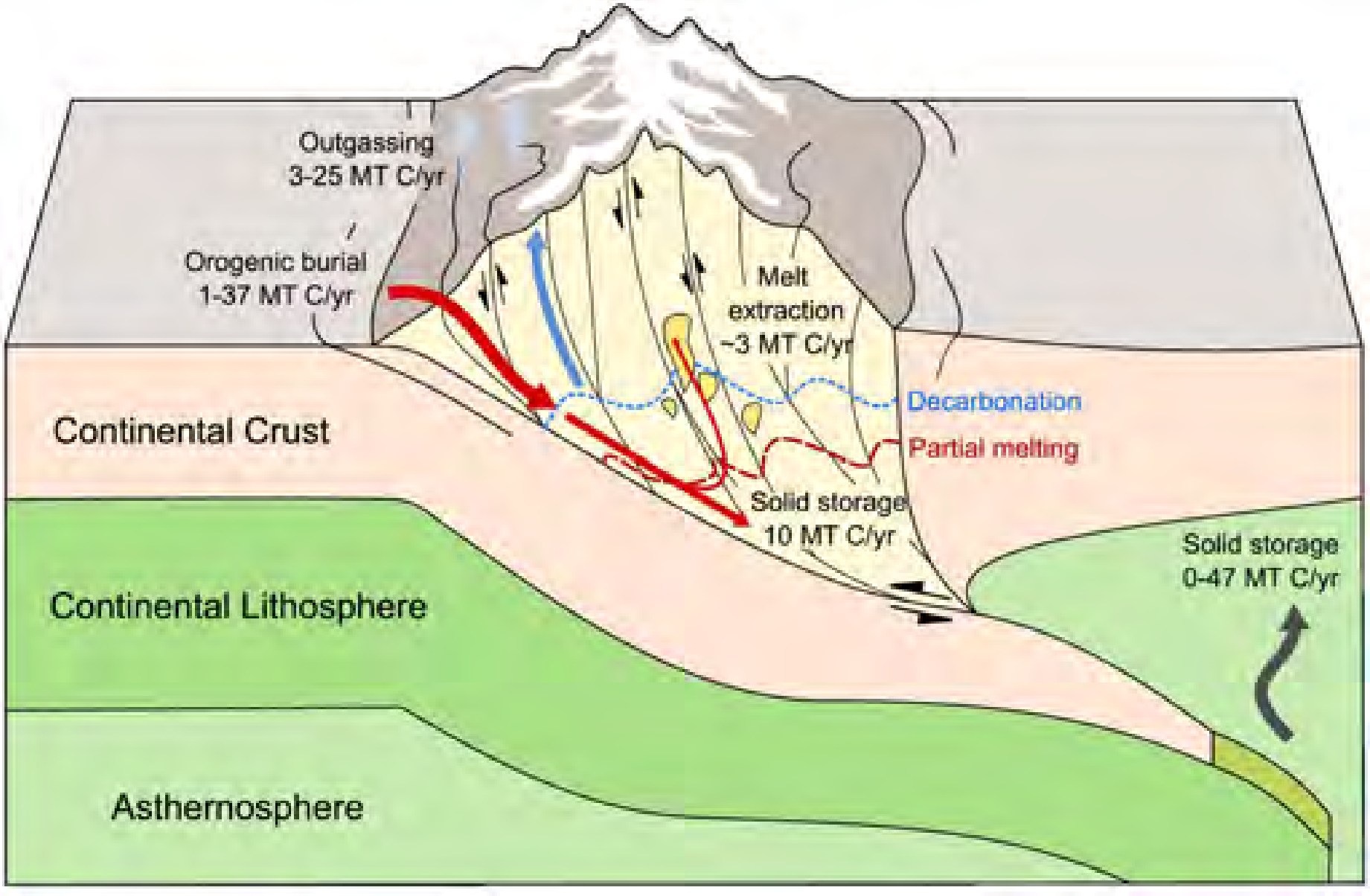
Outgassing
3-25 MT C/yr
Orogenic burial
1-37 MT C/yr
Melt
extraction
~3 MT C/yr
Decarbonation
Partial melting
Solid storage
10 MT C/yr
Solid storage
0-47 MT C/yr
Continental Crust
Continental Lithosphere
Asthenosphere

Figure 6

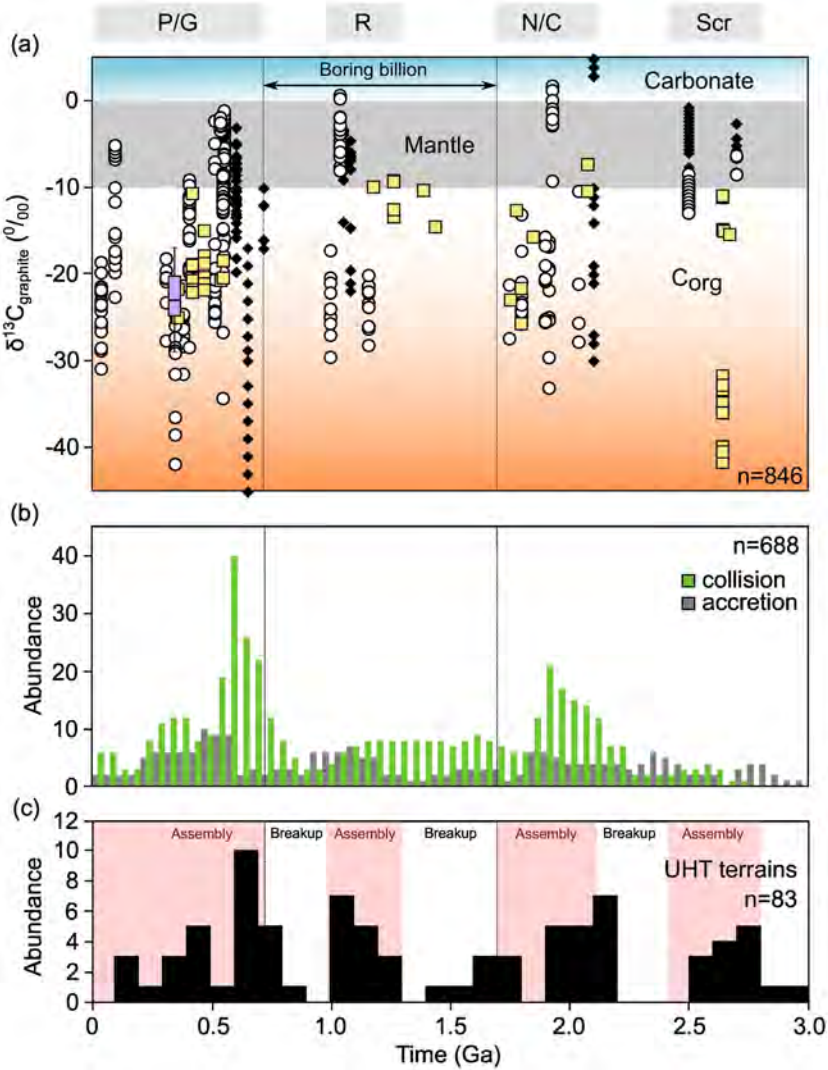
P/G
R
N/C
Scr
(a)
Boring billion
Carbonate
Mantle
Corg
n=846
δ13Cgraphite (0/00)
(b)
n=688
collision
accretion
Abundance
(c)
Assembly
Breakup
Assembly
Breakup
Assembly
Breakup
Assembly
UHT terrains
n=83
Abundance
Time (Ga)

Figure 7

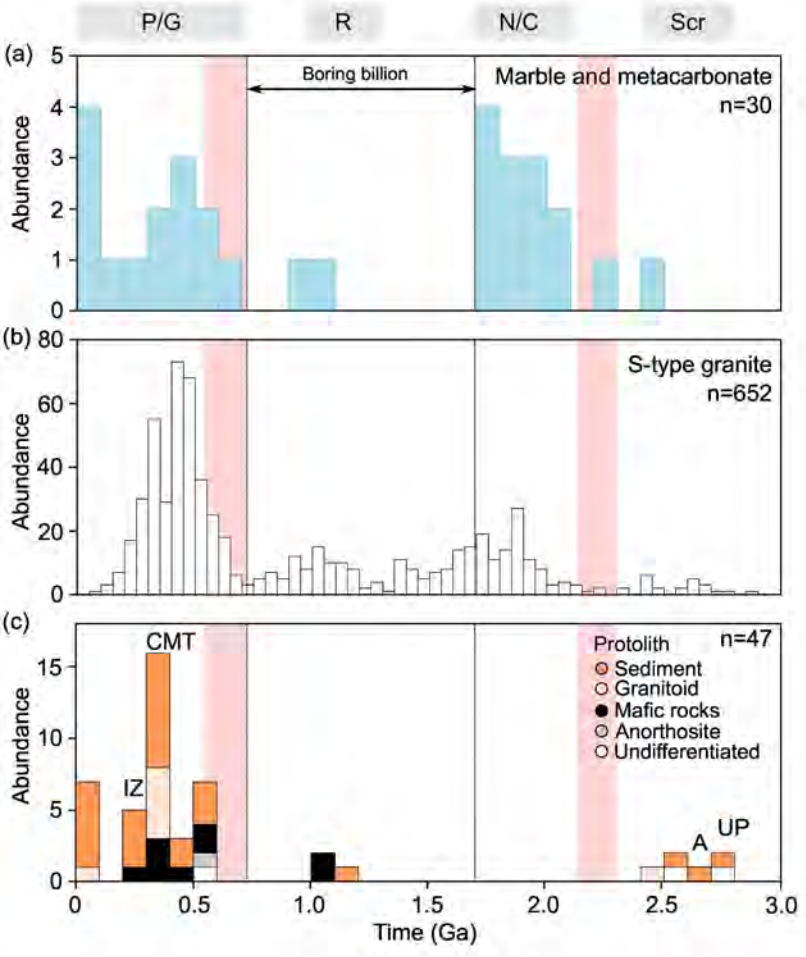
P/G
R
N/C
Scr
(a)
Boring billion
Marble and metacarbonate
n=30
Abundance
(b)
S-type granite
n=652
Abundance
(c)
CMT
IZ
A
UP
Protolith
Sediment
Granitoid
Mafic rocks
Anorthosite
Undifferentiated
n=47
Abundance
Time (Ga)

Figure 8